

Assessment of Kohn-Sham density-functional orbitals as approximate Dyson orbitals for the calculation of electron-momentum-spectroscopy scattering cross sections

Patrick Duffy and Delano P. Chong

Department of Chemistry, The University of British Columbia, 2036 Main Mall, Vancouver, British Columbia, Canada V6T 1Z1

Mark E. Casida and Dennis R. Salahub

Département de Chimie, Université de Montréal, Case Postale 6128, Succursale centre-ville, Montréal, Québec, Canada H3C 3J7

(Received 15 July 1994)

One of the principal advantages of electron momentum spectroscopy (EMS) is that peaks in the binding-energy spectrum can be assigned with greater certainty than in photoelectron spectroscopy, through a comparison of the EMS triple-differential cross sections with the theoretically calculated spherically averaged momentum distributions (MD's) of Dyson orbitals. While the target Hartree-Fock approximation is commonly used to calculate the Dyson orbital MD's for this purpose, a computationally less demanding method would allow the advantages of EMS to be extended to larger molecules. This paper considers the use of Kohn-Sham density-functional theory for this purpose. Although Dyson orbitals are not among the quantities that can be calculated exactly (in the limit of the exact exchange-correlation functional) within the framework of Kohn-Sham density-functional theory, the Kohn-Sham equation can be regarded as an approximate form of Dyson's quasiparticle equation, with a local self-energy. The well known shortcomings of this approach for estimating ionization potentials and band gaps do not *a priori* imply a corresponding problem with the orbitals. After discussing these formal considerations, we introduce the "target Kohn-Sham approximation" as a means of approximating Dyson orbitals by Kohn-Sham orbitals. The quality of this approximation for the calculation of MD's is assessed by comparison with high-quality configuration-interaction calculations, the target Hartree-Fock approximation, and experiment, for several small molecules. The quality of the target Kohn-Sham approximation MD's is found to be comparable to that of the MD's from the target Hartree-Fock approximation, with evident practical implications for EMS.

PACS number(s): 31.20.Sy, 34.80.Gs, 33.10.Cs, 33.60.-q

I. INTRODUCTION

Electron momentum spectroscopy (EMS) is a technique similar to photoelectron spectroscopy but with the important difference that in EMS the target molecule is ionized by an electron rather than by a photon. A detailed study of the kinematics of the incoming electron and two outgoing electrons in this binary ($e, 2e$) scattering experiment allows additional information to be obtained from EMS which cannot now be extracted from photoelectron spectroscopy. Not only can a binding-energy spectrum be obtained in this manner, but the triple-differential cross section for each peak in the binding-energy spectrum can be determined. This cross section is proportional to the spherically averaged momentum distribution (MD) of the Dyson orbital for that ionization event. Comparison of the shapes of the triple-differential cross sections with the MD's from theoretical calculations of the Dyson orbitals thus allows EMS to assign peaks in the binding-energy spectrum with greater certainty than is possible in photoelectron spectroscopy. Once this assignment has been made, quantitative as-

pects of the comparison between the theoretical and experimental MD's provide information on the quality of the theoretically calculated Dyson orbitals. Since the MD's probe primarily the low-momentum region, this technique is particularly useful as a test of the theoretical description of the large- r region.

The theory of EMS has become well established since the birth of the experimental technique roughly a quarter of a century ago [1-13]. Highly accurate Dyson orbitals can be obtained from configuration-interaction (CI) calculations, and the MD's of these Dyson orbitals are in quantitative agreement with experiment. However, this level of accuracy is computationally demanding, nominally scaling as $O(N^5)$ or worse, where N is the size of the basis set. This limits the practical utility of CI for routine EMS calculations to very small molecules. One way around this problem is to use the Hartree-Fock (HF) method to approximate Dyson orbitals, through the "target Hartree-Fock approximation" (THFA). The quality of the resulting MD's is, of course, lower than that obtained from CI calculations, but the accuracy is usually quite adequate for the needs of EMS. Since finite basis set calculations scale nominally as $O(N^4)$, this allows EMS

assignments of peaks in the binding-energy spectrum for larger molecules than is possible with CI calculations, but, especially in view of the need for extended basis sets for calculating MD's, this is still too restrictive to treat many problems of interest to electron momentum spectroscopists. Thus a computationally less demanding method is needed in order to realize the advantages of EMS for larger molecules.

Density-functional theory (DFT) would seem to be a natural choice, since Kohn-Sham (KS) DFT calculations which use an auxiliary basis of $M \propto N$ functions scale nominally as $O(N^3)$, and the quality of the results for a wide variety of properties are generally comparable to or better than Hartree-Fock calculations [14–28]. However, using KS DFT to calculate MD's for EMS is not simply a matter of calculating yet another property from DFT, because it involves using KS DFT to approximate Dyson orbitals. In their formulation of DFT [29], Kohn and Sham introduced orbitals purely as a convenient mathematical construct for simplifying calculations rather than as physically meaningful quantities. The observation that Kohn-Sham orbital energies provide rather poor estimates of ionization potentials and band gaps only seemed to emphasize the fictitious nature of these orbitals. However, there is a formally different approach to DFT in which the *true* Kohn-Sham orbitals (i.e., those that would correspond to the exact exchange-correlation potential) arise as *approximations* to Dyson orbitals [30–33]. Unfortunately, this formal connection says nothing about the quality of the approximation, which must therefore be assessed computationally, as must the effect of the further approximation involved in using Kohn-Sham orbitals obtained from approximate functionals. The formal sense in which the KS orbitals approximate Dyson orbitals (or equivalently Hartree-Fock orbitals, in the exchange-only case), as well as the available numerical evidence, is reviewed in the next section.

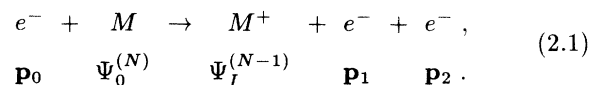
The primary goal of the present paper is to investigate DFT as a potential computational tool for use in EMS. Yet in assessing the quality of MD's obtained from KS orbitals by comparison with those from high-quality CI calculations and with experiment, the present work also makes a small contribution to the larger question of the quality of the approximation of Dyson orbitals by KS orbitals.

II. THEORY

The formal justification for using Kohn-Sham orbitals as approximate Dyson orbitals for use in the theory of electron momentum spectroscopy (EMS) is presented in this section. The theory of EMS is reviewed first, followed by the relevant properties of Dyson orbitals in the context of the quasiparticle equation. The Kohn-Sham density-functional formalism is then summarized, and the section ends with a discussion of the sense in which Kohn-Sham orbitals approximate Dyson orbitals.

A. Electron momentum spectroscopy

Electron momentum spectroscopy is a binary ($e, 2e$) experiment in which an electron with initial momentum \mathbf{p}_0 collides with a neutral molecule M in its ground electronic state $\Psi_0^{(N)}$, knocking out a second electron,



The final state consists of the cation M^+ in its I th excited state $\Psi_I^{(N-1)}$, and two electrons with momenta \mathbf{p}_1 and \mathbf{p}_2 , respectively. The theory of this reaction has been well studied [1,2]. Under symmetric noncoplanar conditions and at high enough impact energies for the plane-wave impulse approximation (PWIA) to be valid, the triple-differential cross section at knockout energy

$$-\omega_I = \frac{p_0^2}{2} - \frac{p_1^2}{2} - \frac{p_2^2}{2} \quad (2.2)$$

and recoil momentum

$$\mathbf{p} = \mathbf{p}_0 - \mathbf{p}_1 - \mathbf{p}_2 \quad (2.3)$$

is given by the generalized overlap approximation (GOA) [1]. (Atomic units are used throughout the present paper, so $\hbar = m = e = 1$.) That is, the triple-differential cross section is proportional to $\Pi(p)$, the spherically averaged momentum distribution (MD) of a Dyson orbital,

$$\Pi(p) = \int |\langle \mathbf{p} | \psi_I \rangle|^2 d\Omega_p, \quad (2.4)$$

where \mathbf{p} here denotes a plane-wave spin orbital with that momentum. The Dyson orbital is given explicitly by the generalized overlap

$$\psi_I(1) = \sqrt{N} \int \int \dots \int \Psi_I^{(N-1)*}(2, 3, \dots, N) \times \Psi_0^{(N)}(1, 2, \dots, N) d2d3 \dots dN, \quad (2.5)$$

where the numerals $i = 1, 2, \dots$ represent the space and spin coordinates of electron i . Strictly speaking, the experimentally measured quantity differs from the triple-differential cross section due to the finite resolution of the experimental apparatus and is therefore referred to as an “experimental momentum profile” (XMP).

The dominant contribution to the MD comes from the large- r part of the orbital [34]. The asymptotic behavior of the most diffuse Dyson orbital is largely determined by the first ionization potential. In the atomic case, the large- r limit for this orbital is given by [34,35]

$$\psi_I(\mathbf{r}\sigma) \rightarrow Cr^{1/\sqrt{-2\omega_I}} e^{-\sqrt{-2\omega_I} r}. \quad (2.6)$$

The link between ionization potentials and the large- r behavior of the other Dyson orbitals is similar but more subtle [34,35]. This link is especially interesting in view of the importance of this region for EMS, since it suggests that the quality of the calculated MD, $\Pi(p)$, may

be correlated with the quality of the ionization potential calculated in this approach.

Dyson orbitals can be obtained either directly, as solutions of Dyson's quasiparticle equation (Sec. IIB), or indirectly, by calculating the N - and $(N-1)$ -electron wave functions (e.g., by CI or many-body perturbation theory calculations) and then obtaining the Dyson orbital as the overlap (2.5). Both approaches give the same result in the limit of a full treatment of correlation (even if the basis set is incomplete [36]). Thus we are free to choose whichever approach is most convenient as a starting point for developing approximate treatments. The one-electron picture used in the quasiparticle equation is often convenient for the development of approximations [36–38], and the quasiparticle equation approach is advantageous for making connections with density-functional theory, as will be discussed in Sec. IID

Highly accurate Dyson orbitals have been calculated via the CI method, using the indirect approach, by Davidson *et al.* [3–13]. While this type of calculation leads to momentum distributions in excellent agreement with measured XMP's, the cost of this level of accuracy is prohibitive for all except very small molecules. Although MD's of Dyson orbitals obtained by direct solution of Dyson's quasiparticle equation have only been calculated using more limited basis sets and lower order treatments of correlation [12,39–42] (see also Ref. [43]), it is clear that both the direct and indirect approaches suffer from similar computational exigencies with regard to the accurate treatment of correlation, including the need to use extended basis sets.

Additional basis functions are also needed for the description of orbitals in the "large- r region" of space far from the nuclei which is important for EMS. Thus these calculations require sufficiently large basis sets to be able to describe both the energetically important small- r region and the large- r region which is so important for EMS but which is relatively unimportant energetically.

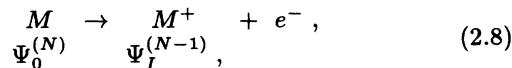
B. Dyson's equation and target approximations

The direct method for obtaining Dyson orbitals and ionization potentials by solving Dyson's quasiparticle equation [44] is reviewed here, as is the important notion of a target approximation. A wave-function-based explanation of Dyson's quasiparticle equation may be found in Ref. [36].

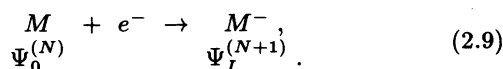
Dyson's quasiparticle equation,

$$\left[\hat{h}_H[\rho] + \hat{\Sigma}_{xc}(\omega_I) \right] \psi_I = \omega_I \psi_I, \quad (2.7)$$

simultaneously describes vertical ionization of the molecule M ,



and electron attachment,



Here,

$$\hat{h}_H[\rho] = -\frac{1}{2}\nabla^2 + v(\mathbf{r}) + \int \frac{\rho(2)}{|\mathbf{r} - \mathbf{r}_2|} d2 \quad (2.10)$$

is the usual Hartree Hamiltonian expressed in terms of the density ρ , and v is just the nuclear attraction potential (plus the external field, if any). The term $\hat{\Sigma}_{xc}(\omega)$ is the exchange-correlation (xc) self-energy operator which includes many-body effects such as correlation and relaxation [43] and dynamic polarization [37,38] as well as a correction for the self-interaction error in the Coulomb part of the Hartree Hamiltonian. Dyson's equation is a generalized eigenvalue problem whose solutions fall into two classes. If the I th ionization potential and electron affinity are denoted by \mathcal{I}_I and \mathcal{A}_I , respectively, the "ionization solutions" satisfy

$$\omega_I = -\mathcal{I}_I, \quad (2.11)$$

$$\begin{aligned} \psi_I(1) = & \sqrt{N} \int \int \dots \int \Psi_I^{(N-1)*}(2, 3, \dots, N) \\ & \times \Psi_0^{(N)}(1, 2, \dots, N) d2 \dots dN, \end{aligned} \quad (2.12)$$

while the "electron affinity solutions" satisfy

$$\omega_I = -\mathcal{A}_I, \quad (2.13)$$

$$\begin{aligned} \psi_I(1) = & \sqrt{N+1} \int \int \dots \int \Psi_I^{N*}(2, 3, \dots, N+1) \Psi_0^{(N+1)} \\ & \times (1, 2, \dots, N+1) d2 \dots d(N+1). \end{aligned} \quad (2.14)$$

There are an infinite number of Dyson orbitals ψ_I , and their norms, i.e., the spectroscopic factors S_I , may be calculated from the energy derivative of the xc self-energy,

$$S_I = \langle \psi_I | \psi_I \rangle = \left[1 - \frac{\langle \psi_I | \hat{\Sigma}'_{xc}(\omega_I) | \psi_I \rangle}{\langle \psi_I | \psi_I \rangle} \right]^{-1}. \quad (2.15)$$

Dyson's equation must be solved self-consistently because the xc self-energy $\hat{\Sigma}_{xc}(\omega_I)$ is a function of the orbital energy ω_I and the Hartree Hamiltonian $\hat{h}_H[\rho]$ depends upon the orbitals through

$$\rho(1) = \sum_I^{\text{ionization}} |\psi_I(1)|^2. \quad (2.16)$$

The HF equation is a limiting case of Dyson's equation where the self-energy is approximated by its exchange-only part,

$$\hat{\Sigma}_x^{\text{HF}} \chi(1) = - \sum_i^{\text{ionization}} \psi_i^{\text{HF}}(1) \int \frac{\psi_i^{\text{HF}*}(2) \chi(2)}{r_{12}} d2, \quad (2.17)$$

defined here by its action on an arbitrary function χ . Since this self-energy is independent of ω , the Dyson orbitals are normalized to unity [Eq. (2.15)] in the HF ap-

proximation. It then follows [Eq. (2.16)] that the integral of the density ρ gives the number of ionization solutions. Hence, since the density integrates to the number of electrons, there must be exactly one ionization solution (i.e., exactly one occupied orbital) for each electron. The approximation of the ionization potentials by the negative of the Hartree-Fock orbital energies is the Koopmans ionization potential,

$$\omega_i \approx \epsilon_i^{\text{HF}}. \quad (2.18)$$

The frozen-orbital approximation (FOA) consists of taking the Dyson orbitals to be HF orbitals,

$$\psi_i \approx \phi_i^{\text{HF}}. \quad (2.19)$$

Note that, at this level of approximation, the index I , which labels the many-electron state of the daughter ion formed, can be replaced by the label i of the orbital out of which ionization occurs. The FOA is qualitatively incorrect. Since it gives only N Dyson orbitals, all normalized to unity, it cannot account for the existence of “satellites,” nor for the intensities, in the binding-energy spectrum.

While the HF approximation has some value in describing outer valence ionization, more elaborate and accurate self-energy approximations [45–50] are needed to describe the complex many-body phenomena seen in inner valence ionization spectra [4–13]. The corrections to the HF independent-particle picture of ionization which arise from the use of better self-energy approximations may be analyzed using simple Rayleigh-Schrödinger perturbation theory [43,51]. Any independent-particle Schrödinger equation

$$\hat{h}\phi_i = \epsilon_i\phi_i \quad (2.20)$$

can serve as the zero-order approximation. While the HF equation is the usual choice in the molecular literature [45,48,49,50,51], the Kohn-Sham equation is often used in the solid-state literature [52–58]. Once a choice is made, Dyson’s equation can be rewritten as

$$\left\{ \hat{h} + \left[\hat{\Sigma}_{\text{xc}}(\omega_I) - \hat{w} \right] \right\} \psi_I(1) = \omega_I \psi_I(1), \quad (2.21)$$

where

$$\hat{w} = \hat{h} - \hat{h}_H. \quad (2.22)$$

Note that $\hat{w} = v_{\text{xc}}$ if the zero-order Hamiltonian is the Kohn-Sham Hamiltonian, and that $\hat{w} = \hat{\Sigma}_x^{\text{HF}}$ if the zero-order Hamiltonian is the Hartree-Fock Hamiltonian and differences between the true and Hartree-Fock densities are ignored. Once again, the index I labels a many-electron ion state while the index i labels an orbital. The nonlinear nature of Dyson’s equation means that many I ’s can correspond to the same i . For each zero-order solution $\{\epsilon_i, \phi_i\}$, the first-order equation

$$\omega_I^{(i)} = \epsilon_i + \langle \phi_i | \hat{\Sigma}_{\text{xc}}(\omega_I^{(i)}) - \hat{w} | \phi_i \rangle \quad (2.23)$$

can be solved for a set of $\omega_I^{(i)}$. This corresponds to the

experimentally observed fractionation of principal ionization transitions into many “satellite” processes. Each value of $\omega_I^{(i)}$ can then be used to generate a first-order solution for the corresponding Dyson orbital and spectroscopic factor,

$$\tilde{\psi}_I^{(i)} = \phi_i + \sum_r^{\epsilon_r \neq \epsilon_i} \phi_r \frac{\langle \phi_r | \hat{\Sigma}_{\text{xc}}(\omega_I^{(i)}) - \hat{w} | \phi_i \rangle}{\epsilon_i - \epsilon_r}, \quad (2.24)$$

$$S_I^{(i)} = \left[1 - \langle \phi_i | \hat{\Sigma}'_{\text{xc}}(\omega_I^{(i)}) | \phi_i \rangle \right]^{-1}, \quad (2.25)$$

where

$$\tilde{\psi}_I^{(i)} = \psi_I^{(i)} / \sqrt{S_I^{(i)}} \quad (2.26)$$

is a *renormalized Dyson orbital*. Since the derivative $\langle \phi_i | \hat{\Sigma}'_{\text{xc}}(\omega_I^{(i)}) | \phi_i \rangle \leq 0$, Eq. (2.25) indicates that the spectroscopic factors are less than 1, though spectroscopic factors near unity are typical for the outer valence region where the self-energy is normally a relatively slowly varying function of energy.

Most of these features are preserved in the simpler “target approximation” commonly used to analyze EMS experiments. This simply assumes that the first-order terms in Eq. (2.24) can be neglected, with the result that the renormalized Dyson orbital $\tilde{\psi}_I^{(i)}$ is approximately equal to ϕ_i , or equivalently

$$\psi_I \approx \sqrt{S_I^{(i)}} \phi_i. \quad (2.27)$$

Since the HF approximation is the zero-order approximation generally used for this purpose, this is usually called the “target Hartree-Fock approximation” (THFA) [1]. An important consequence of the target approximation follows from the fact that the occupation number $n[\chi]$ of any orbital χ can be evaluated as an expectation value of the one-electron reduced density matrix γ ,

$$n[\chi] = \int \int \chi^*(1) \gamma(1, 1') \chi(1') d1 d1', \quad (2.28)$$

using the expression for the density matrix in terms of Dyson orbitals,

$$\gamma(1, 1') = \sum_I^{\text{ionization}} \psi_I(1) \psi_I^*(1'). \quad (2.29)$$

Combining the target approximation [Eq. (2.27)] with these expressions gives

$$n[\phi_i] = \sum_I^{\text{ionization}} S_I^{(i)}, \quad (2.30)$$

which is close to unity in most cases,

$$\sum_I^{\text{ionization}} S_I^{(i)} \cong 1. \quad (2.31)$$

This allows the experimental determination of spectro-

scopic factors in the following fashion. First a zero-order orbital ϕ_i is assigned to each observed binding energy by comparison of the *shape* of the XMP at that binding energy with that from the theoretically calculated MD. The spectroscopic factors $S_I^{(i)}$ can then be assigned from the relative intensities of the XMP's associated with the same zero-order orbital, using the "normalization" relation (2.31).

Although Eq. (2.27) is reminiscent of the FOA, the target approximation is in fact qualitatively much more similar to the first-order solution of Dyson's equation. In the FOA, each occupied orbital ϕ_i corresponds to a single observable ionization transition with a spectroscopic factor of unity and an ionization potential ($-\epsilon_i$). In contrast, the target approximation allows the ionization process to be decomposed into several transitions $\omega_I^{(i)}$, given by Eq. (2.23), each with spectroscopic factors less than unity [Eq. (2.25)], consistent with the picture arising from the perturbation analysis of Dyson's equation and with the experimentally observed facts.

C. Kohn-Sham density-functional theory

Kohn-Sham (KS) density-functional theory (DFT) is a computationally less demanding alternative to conventional *ab initio* electronic structure methods. The KS formalism is briefly summarized here with emphasis on similarities and differences between the KS equation and Dyson's equation. More complete reviews of DFT can be found in Refs. [59–61].

Basing their method on an existence proof due to Hohenberg and Kohn [62], Kohn and Sham [29] proposed determining the total energy E and density ρ of a system of N interacting electrons in an external potential v by minimizing a functional which we shall write in its spin-density variant as

$$E[\rho] = -\frac{1}{2} \sum_{i=1}^N \langle \phi_i^{\text{KS}} | \nabla^2 | \phi_i^{\text{KS}} \rangle + \int v(\mathbf{r}_1) \rho(1) d1 + \frac{1}{2} \int \int \frac{\rho(1)\rho(2)}{r_{12}} d1d2 + E_{\text{xc}}[\rho], \quad (2.32)$$

where the KS orbitals ϕ_i^{KS} have been introduced as the orbitals of a fictitious system of noninteracting electrons whose densities sum to the exact total density,

$$\rho(1) = \sum_{i=1}^N |\phi_i^{\text{KS}}(1)|^2. \quad (2.33)$$

Note that $\rho(1)$ depends on both the space and spin coordinates of electron 1; hence $E_{\text{xc}}[\rho] = E_{\text{xc}}[\rho^\uparrow, \rho^\downarrow]$ is a spin-density functional. The four terms in Eq. (2.32) represent, respectively, (i) the kinetic energy of a fictitious system of noninteracting electrons with orbitals ϕ_i^{KS} , (ii) the potential energy of the electrons in the external potential (i.e., the nuclear attraction potential in molecular applications), (iii) the Coulomb repulsion energy, and (iv) the "exchange-correlation (xc) energy" (which includes both a correction for the self-interaction error in

the Coulomb term and the difference between the kinetic energies of the true interacting and fictitious noninteracting systems, as well as exchange and correlation.) No computationally practical exact form is yet known for the xc energy, so this term is approximated in practice. Minimization of the total energy subject to the constraint of orthonormal orbitals gives the Kohn-Sham equation

$$(\hat{h}_H[\rho] + v_{\text{xc}}(1; \rho)) \phi_i^{\text{KS}}(1) = \epsilon_i^{\text{KS}} \phi_i^{\text{KS}}(1), \quad (2.34)$$

where

$$v_{\text{xc}}(1; \rho) = \frac{\delta E_{\text{xc}}[\rho]}{\delta \rho(1)} \quad (2.35)$$

is the KS xc potential. (The notation $v_{\text{xc}}(1; \rho)$ means that v_{xc} is a function of the space and spin coordinates of electron 1 and a functional of ρ .) Note that $v_{\text{xc}}(1)$ is a local potential (i.e., just a multiplicative operator), though $v_{\text{xc}}(1; \rho)$ may be either a local or a nonlocal functional of ρ . Equation (2.34) is precisely the orbital Schrödinger equation for the KS fictitious system of noninteracting electrons.

It is useful to make a distinction between exact DFT and the approximate DFT necessarily used in practical calculations. In exact DFT, the xc potential is (by definition) the local potential whose orbital densities sum to the exact total density of the interacting system. In contrast, practical KS DFT uses approximate functionals which contain errors affecting the xc potential and hence the calculated orbitals, orbital energies, charge density, and total energy. Exact DFT is not merely a hypothetical construct. Sham and Schlüter observed that the definition of the exact v_{xc} permits the calculation of "exact" xc potential functions (but not functionals) from densities obtained in many-body Green function calculations [32,63–68], thereby allowing the study of the exact KS orbitals and orbital energies. This may also be done via the optimized-effective-potential (OEP) approach [31,69–80]. The concept of exact DFT is useful for purposes of distinguishing between properties or limitations inherent in DFT and those arising from the quality of an approximate functional. The discussion in this and the following subsection will be in terms of exact DFT.

There is an obvious superficial resemblance between the KS equation and Dyson's quasiparticle equation. However, while the KS equation is the orbital equation for a fictitious system of noninteracting particles moving in the local potential $[v + \int \rho(2)/r_{12} d2 + v_{\text{xc}}]$, Dyson's equation refers to quasiparticles moving in a potential with an orbital energy-dependent nonlocal contribution $\hat{\Sigma}_{\text{xc}}(\omega_I)$. Consequently, there are only N orthonormal KS orbitals, while the Dyson orbitals are neither orthogonal, nor normal, nor finite in number. Nevertheless, the two equations share a few properties in common which are worth pointing out. Both have orbital solutions whose densities sum to the exact total density [Eqs. (2.16) and (2.33)]. This alone indicates that the KS and Dyson orbitals can differ by no more than a phase factor in regions of space dominated by only a single orbital from each set. In particular, this must be true for the highest occupied molecular orbital (HOMO) in the large- r limit, since all other orbitals must die off more quickly [34,35],

$$\frac{|\phi_{\text{HOMO}}^{\text{KS}}(1)|^2}{|\psi_{\text{HOMO}}(1)|^2} \xrightarrow{r \rightarrow \infty} 1. \quad (2.36)$$

A corollary [35] which follows from examination of the asymptotic behavior of the charge density is that both the KS and Dyson HOMO energies must equal the negative of the first ionization potential provided the orbital energy zero is chosen so that the xc potential vanishes asymptotically. The equality of the KS and Dyson HOMO energies is an example of a property which holds for exact DFT but which is generally not found in practical DFT calculations with the approximate functionals presently available.

D. Approximate Dyson orbitals from DFT

The computational advantages of DFT make it an attractive possibility for the calculation of MD's for use with EMS. However, the question of principle regarding the use of KS orbitals to approximate Dyson orbitals should be addressed first. This is properly done in the framework of exact DFT.

It is widely appreciated that, in the KS approach to DFT, the orbitals of a fictitious noninteracting system were introduced purely as a formal device to facilitate the treatment of the kinetic energy functional. Thus, Kohn and Sham did not consider these orbitals to be physically meaningful. This view seemed to be corroborated by the fact that the eigenvalues of the KS equation were found not to be good approximations for the ionization potentials and electron affinities, a problem which is most pronounced when approximate functionals are used but which persists in exact KS DFT [66,77,81].

However, there is another approach to DFT in which the KS equation is derived as an approximation to Dyson's quasiparticle equation. This is an outgrowth of Slater's initial concept [82] of v_x as a local approximation to the nonlocal exchange operator in the Hartree-Fock approximation. From this point of view, there is no reason to think that the KS orbitals should be devoid of physical significance. In this approach, one starts with Dyson's equation and finds the local (in both space and time) potential which best approximates $\hat{\Sigma}_{xc}(\omega)$, in a well-defined variational sense. The resulting potential is known as the optimized effective potential (OEP). In their seminal paper, Sharp and Horton [30] and subsequently Talman and Shadwick [31] gave an expression for this OEP in the exchange-only case. Casida [33] has recently generalized this approach to treat the correlated case as well. In both cases, the resulting OEP can be identified with the exact KS v_{xc} (or v_x) derived by Sham and Schlüter¹ [32,33]. Thus, the KS equation is the vari-

tionally best local approximation to Dyson's quasiparticle equation, so in this sense it is natural to consider KS orbitals and orbital energies as approximate Dyson orbitals and orbital energies. Note that, unlike the total energy and charge density, the individual Dyson orbitals and orbital energies are not among the quantities which are obtained exactly in "exact" KS DFT; it is the *true* KS orbitals and orbital energies which here arise as *approximations* to the Dyson orbitals and orbital energies. The question then becomes whether this approximation is good enough to be useful.

The shortcomings of the KS orbital energies as approximate Dyson orbital energies are well known. Indeed, Perdew and Levy [86] have pointed out this is to be expected on the basis of derivative discontinuities in the xc energy functional. However, this difficulty with the orbital energies does not imply that the KS orbitals are necessarily poor approximations to the Dyson orbitals. While it may seem counterintuitive that the KS orbitals could be good approximations to the Dyson orbitals when this is not true for the corresponding orbital energies, the qualitative description of the localization process given in the Appendix suggests that, even if the Dyson orbitals were directly proportional to KS orbitals, the corresponding eigenvalues should differ in order to produce an orbital-independent local potential v_{xc} .

Unfortunately, these formal considerations do not give any *a priori* statement as to the quality of the approximation of Dyson orbitals by KS orbitals, nor any limiting case in which it becomes exact. In order to obtain an idea of the quality of this approximation, we consider the available numerical data from exact DFT calculations. First the exchange-only case. In this case, one measure of the quality of the OEP (or exact KS) orbitals as approximate HF orbitals is how well they minimize the HF energy expression. That is, the difference between the HF energy expression evaluated with OEP orbitals and the true HF energy provides a measure of the severity of the local approximation. Explicit calculations on atoms show that this energy difference ranges from about 50 ppm for the lightest atoms to about 5 ppm for atoms with atomic numbers near 50 [72,77]. This and other calculated properties [69,70] such as impulse Compton profiles, atomic form factors, $\langle r^2 \rangle$, and dipole polarizabilities, as well as orbital properties [72] such as $\langle r \rangle$, $\langle r^2 \rangle$, $\langle 1/r \rangle$, and $\langle 1/r^3 \rangle$ indicate that the exchange-only Kohn-Sham orbitals are remarkably close to HF orbitals. A similar conclusion was reached by Zhao and Parr [87,88] in their direct comparison of exact (exchange-only) atomic KS orbitals with the corresponding HF orbitals. Although much less information is available in the exchange-correlation case, some information is available from Green function calculations on solids [52,53,55], though this is not from exact DFT. These begin with KS DFT calculations using the local density approximation (LDA) for the xc energy as the zero-order description, and then follow up by solving Dyson's quasiparticle equation using the *GW* (i.e., Green function G times screened interaction W) approximation [89] for the xc self-energy. Overlaps of 99.9% between the KS and renormalized Dyson orbitals are found in these calculations. Thus the numerical evidence is that KS or-

¹This identification holds within the linear response approximation to the Sham-Schlüter equation (see Ref. [33]). This approximation is routinely used in calculations of the exact v_{xc} (or v_x), and its acceptance is implicit in the acceptance of OEP calculations as giving the exact KS $x(c)$ potential [31,66,67,69–81,83–85].

bitals can serve as good approximations for renormalized Dyson orbitals.

Now let us clarify the precise sense in which we intend KS orbitals as approximate Dyson orbitals. Just as in the HF approximation, there are only N KS orbitals, as opposed to an infinite number of Dyson orbitals, and the considerations in Sec. IIB on the frozen-orbital versus target approximations apply equally to DFT and the HF approximation. Thus what we are proposing is a target Kohn-Sham approximation (TKSA) in which each ionization Dyson orbital is taken to be proportional to an occupied (canonical) Kohn-Sham orbital [Eq. (2.27)]. The TKSA is expected to break down when the perturbation $[\hat{\Sigma}_{xc}(\omega_I) - v_{xc}]$ becomes too large. However, just as with the target Hartree-Fock approximation (THFA), this breakdown is most likely to occur for energies ω_I where the self-energy is varying rapidly, in which case the spectroscopic factor will be small [Eq. (2.25)] and the transition will be difficult to observe experimentally.

As was remarked in Sec. IIA, Dyson orbitals may be calculated either directly, as solutions of the quasiparticle equation, or indirectly via the generalized overlap formula (2.5). Since both approaches yield the same result in the limit of an exact treatment of many-body effects, either one may be used as a starting point for approximations to the Dyson orbital. We have chosen to use the former (quasiparticle equation) approach, since it lends itself more readily to approximation via DFT. The latter (generalized overlap) approach would have required introducing an N -particle wave function in the DFT treatment, as well as doing DFT calculations on excited states of the daughter ion, with all its attendant formal and practical difficulties. Or, in order to avoid the problems of excited states, one would need some sort of Koopmans-like theorem for DFT, relating the generalized overlap to the parent KS orbitals, but no such theorem has been proven to date. In contrast, the approach we have taken in this paper is based entirely on the quasiparticle equation. The self-energy is approximated through a localization (OEP) procedure which yields the KS equation. Thus the (canonical) KS orbitals are just the solutions of this approximate quasiparticle equation, and, in this sense, approximate Dyson orbitals. This point of view has the advantage that the aforementioned problems with the generalized overlap approach are not encountered.

Although, in the case of an exact self-energy, the generalized overlap yields the same Dyson orbital as is obtained by solving the quasiparticle equation, this need not always be the case for an approximate self-energy. The generalized overlap and the solution of the quasiparticle equation are then equally justified, but possibly different, approximations to the true Dyson orbital. Nevertheless, it is interesting, for purposes of clarifying the physical picture implied by a given self-energy approximation, to try to understand the relationship between the generalized overlaps and the solutions of the quasiparticle equation, within this self-energy approximation. This relationship is not yet clear in the case of DFT.

In addition to the TKSA whose formal justification has just been discussed, two *ad hoc* DFT approximations of Dyson orbitals are also considered in this paper, in order

to illuminate different points, each of which might naïvely appear to offer some advantages.

The first *ad hoc* approach is based on analogy with the Hartree-Fock approximation. In the Hartree-Fock approximation, Koopmans' theorem provides the relation between the solutions of the quasiparticle equation and the generalized overlaps. Since the Hartree-Fock method consists of approximating the exchange-correlation self-energy $\hat{\Sigma}_{xc}$ by the HF exchange operator $\hat{\Sigma}_x$, the (canonical) HF orbitals, being solutions of this approximate quasiparticle equation, approximate Dyson orbitals. Koopmans' original formulation [90] of the theorem that bears his name concerns a special case in which the generalized overlap is also equal to the canonical HF orbital—namely, when the problem is restricted to the space of the occupied molecular orbitals of the parent species. Then the orbital describing the hole in the daughter ($N - 1$)-electron HF wave function is identical to a canonical HF orbital of the N -electron parent. Although no variant of Koopmans' theorem has been proven for Kohn-Sham density-functional theory, it is interesting to ask what happens if the Kohn-Sham problem of the daughter is solved in the restricted space of the parent occupied KS orbitals. We term the orbital describing the resulting hole, the “Kohn-Sham Koopmans' hole” (KSKH) orbital. Since these KSKH orbitals are related to the canonical KS orbitals by a unitary transformation, they are still KS orbitals, though not necessarily canonical ones. Symmetry arguments alone suffice to show that for any occupied orbital whose symmetry representation is unique among the occupied orbitals (termed “lone symmetry states” in Ref. [43]), this KSKH orbital is identical to the canonical KS orbital. The question is how similar these orbitals are in the absence of such symmetry constraints, and whether this hole (i.e., the KSKH orbital) provides any better description of the Dyson orbital than does the canonical KS orbital. This KS Koopmans' hole approach still involves the formal difficulty of calculating excited states in DFT (see, e.g., Ref. [59], p. 204, and Ref. [60], p. 32). Nevertheless, the analogy with the HF approximation is interesting.

The second *ad hoc* approach returns to the quasiparticle equation (rather than the generalized overlap) point of view, and is aimed at improving the KS eigenvalues as approximations to the eigenvalues of Dyson's equation. As noted previously, the large- r behavior of orbitals plays an important role in their MD's, and this behavior is intimately related to the eigenvalue in Dyson's equation [Eq. (2.6)]. This relationship also holds between the large- r behavior of the KS orbitals and their eigenvalues. While this is no problem for the HOMO where the Dyson equation eigenvalues and the exact KS eigenvalues are both equal to minus the first ionization potential, the eigenvalues and hence the asymptotic behavior of the other Dyson and KS orbitals are expected to differ. Note also that even the HOMO KS eigenvalue is rarely a good approximation to minus the first ionization potential in practical calculations using approximate functionals. The Slater-Janak transition state method [91,92], which consists of solving the KS equations with half an electron removed from the i th orbital, is a well known

way to modify the KS equation so that the i th eigenvalue provides a better approximation to the i th principal ionization potential. (See, e.g., Ref. [93] for an assessment of the transition state method for calculating ionization potentials.) If “better” eigenvalues, in the sense of giving better ionization potentials, imply better orbital behavior in the asymptotic region, then using this “transition orbital” (i.e., the half-occupied orbital resulting from a transition state calculation) might be a useful trick for calculating MD’s for use with EMS. We will refer to this as the “transition orbital method” (TOM).

The discussion in this section has been in terms of exact DFT. However, since we are interested in the question of the practical utility of the approximations discussed for calculating MD’s for EMS, our computational investigation of the approximations presented here necessarily uses approximate functionals. It should be kept in mind that this introduces a further approximation beyond that involved in approximating Dyson orbitals by KS orbitals.

III. COMPUTATIONAL DETAILS

All density-functional calculations reported in this paper were carried out with the computer program deMon [94–96] and will be compared with the highly accurate multireference singles and doubles configuration-interaction (CI) calculations of Davidson and co-workers [3–5,9,10,12,13], who used the program MELD [97]. In order to avoid complicating our comparison between KS, CI, and HF MD’s with differences arising from the geometries, the present work uses the geometries of Davidson *et al.*

deMon belongs to the family of density-functional programs which use Gaussian orbital basis sets. This has the advantage that the same orbital basis sets can be used as in traditional quantum chemistry programs. The integral evaluation in deMon is carried out analytically through the use of two auxiliary basis sets, one for fitting the charge density (used in evaluating the Coulomb integrals) and the other for fitting the xc potentials and xc energy density. The coefficients of each of these expansions are obtained from a least squares fit, which involves a grid in the case of the xc potentials and xc energy density (but not for the charge density fit). Thus the fit quality depends both upon the quality of the grid and on the choice of auxiliary basis sets. The auxiliary basis sets both consist of Gaussian primitives, and are collectively described by the notation $(n, m; n, m)$, where, in each pair, n denotes the number of s -type Gaussians, and m denotes the number of “shells” of s -, p -, and d -type Gaussians sharing the same exponent.

The present calculations use the (4,4;4,4) (heavy atoms) and (3,1;3,1) (hydrogen) auxiliary basis sets, which are the best presently available in the deMon library file. The grid used was extrafine and random, and the self-consistent field (SCF) convergence criterion was five successive energy differences of less than 10^{-8} a.u. The ion calculations done for the KSKH and TOM orbitals were started from the parent density, and were converged to five successive energy differences of less than

10^{-6} a.u. The polarizabilities reported in this work were calculated by finite difference, with a field strength of ± 0.0005 a.u. using the polarizability option in deMon. The MD’s (spherically averaged orbital momentum distributions) were calculated from the orbitals using the in-house HEMS (H-compiler-optimized electron momentum spectroscopy) program of Ref. [98].

Several exchange and correlation functionals were employed in this study; these will be distinguished using the abbreviations LDA_x, LDA_{xc}, B88_x, and B88_x+P86_c. The “x” refers to the exchange functional while “c” refers to the correlation functional, so the LDA_x and B88_x functionals are exchange-only approximations.

The local density approximation (LDA) is the simplest and most widely used functional in the density-functional literature. In the LDA_{xc} functional, the exchange-correlation energy density at each point in the molecule is approximated by that of a homogeneous electron gas whose charge density is the same as the density at that point in the molecule. Specifically,

$$E_{xc}[\rho^\uparrow, \rho^\downarrow] = \int \epsilon_{xc}(\rho^\uparrow(\mathbf{r}), \rho^\downarrow(\mathbf{r}))\rho(\mathbf{r}) d\mathbf{r} \quad (3.1)$$

where $\epsilon_{xc}(\rho^\uparrow(\mathbf{r}), \rho^\downarrow(\mathbf{r}))$ is the exchange-correlation energy density for the homogeneous electron gas with spin densities $\rho^\uparrow(\mathbf{r})$ and $\rho^\downarrow(\mathbf{r})$ and total charge density $\rho(\mathbf{r}) = \rho^\uparrow(\mathbf{r}) + \rho^\downarrow(\mathbf{r})$. In the exchange-only case, this reduces to a simple closed form (the LDA_x functional), identical to Slater’s $X\alpha$ approximation with $\alpha = 2/3$ [99]. A closed form for the correlation part is not known. Instead, the parametrization of Vosko, Wilk, and Nusair [100], is used in deMon.

The LDA neglects any dependence on the gradients of the density, and is therefore most justified for slowly varying densities, though its range of applicability is actually much wider than this would suggest. The next higher level of approximation consists of adding gradient correction terms to the LDA exchange-correlation energy density. One of the most important shortcomings of the LDA is that it tends to overbind molecules [101], and many gradient-corrected functionals were designed with this in mind. In principle, gradient corrections should also improve the results for other properties besides binding energies, though in practice this varies depending on the functional and the property in question. Since the large- r behavior of orbitals is very important for the calculation of properties such as polarizabilities, and MD’s for EMS, it is worth noting that the LDA_x and LDA_{xc} potentials and energy densities violate the known asymptotic behavior of the exact functionals. The 1988 gradient-corrected exchange functional of Becke [102] is an improvement in this regard, being specifically designed so that the exchange energy density ϵ_x has the correct asymptotic behavior, although the same cannot be said for the resulting B88_x potential. However, the asymptotic behavior of the B88_x potential is an improvement on that of the LDA_x potential. The gradient corrections used in the present work are the B88_x functional, for exchange, and the 1986 correlation functional of Perdew [103] (P86_c). The P86_c functional

is based upon a comparison of wave-vector analyses for the correlation energy density of molecules and the homogeneous electron gas [103].

The orbital basis sets used in this work are described below. All consist of contractions of Gaussian-type orbitals (GTO's), and use sets of six Cartesian d functions.

STO-3G. This minimal basis set, due to Hehre, Stewart, and Pople [104], is of single- ζ quality, and consists of a single contraction of three Gaussian primitives for each atomic orbital.

STO-3G#. The # symbol designates the addition of a single set of diffuse p functions to the oxygen basis set in the H_2O calculation. The exponent used is that given by Casida and Chong [34] in their study of the relation between MD's and large- r behavior.

NM. This basis set, designed by Neuman and Moscovitz [105], is of roughly triple- ζ plus polarization quality on oxygen and double- ζ plus polarization quality on hydrogen. It consists of a $(10s6p2d) \rightarrow [5s3p1d]$ contraction on oxygen and a $(4s1p) \rightarrow [2s1p]$ contraction on hydrogen.

TZP. This consists of the $(7111/411/1^*)$ (i.e., $[4s3p1d]$) (oxygen) and $(41/1^*)$ (i.e., $[2s1p]$) (hydrogen) library basis sets of deMon. Here, TZP stands for "triple- ζ plus polarization," although it would be better described as "valence triple- ζ plus polarization" on oxygen and "double- ζ plus polarization" on hydrogen.

ANO-. The atomic natural orbital (ANO) basis sets of Ref. [106] were truncated to d functions on the heavy atoms for use in the present study, since deMon is not yet able to use higher angular momentum atomic orbitals. To maintain balance in the basis sets, the hydrogen set was truncated to p functions. The resulting basis sets consist of five s contractions, four p contractions, and three d contractions on the heavy atoms, and four s and three p contractions on hydrogen.

NHF-. The near Hartree-Fock (NHF) quality 109-GTO basis set of Ref. [4], for water, was truncated to d functions on oxygen and p functions on hydrogen. Sets of six Cartesian d functions were used in the present study, instead of the sets of five d functions used in Ref. [4]. The resulting basis set consisted of 92 contractions of GTO's.

TZP+, ANO+, NHF+. The "+" indicates augmentation of the substrate (TZP, ANO-, or NHF-) basis with the field-induced polarization (FIP) functions of Zeiss *et al.* [107] as described in Ref. [26] (s and d on the heavy atoms and p on hydrogen). However, due to linear dependencies encountered in the case of ANO+, only the d and not the s FIP for the heavy atoms was added in forming the ANO+ and NHF+ basis sets. The ANO+ basis sets were used for most of the calculations reported in this work.

Table I shows the basis set dependence of the total energies, dipole moments, and polarizabilities obtained for H_2O , using deMon with the LDaxc functional. The total energy decreases as the basis set size increases and appears to be converging to about -75.913 hartrees. This is well above the best experimental estimate of the total energy, namely -76.434 hartrees. Although the KS equations are derived by a variational minimization of an energy functional and finite basis calculations of the total

energy should converge from above to the KS value for the functional used, the use of approximate functionals in practical DFT programs means that, unlike the case in HF and CI calculations, the total energy may fall either above or below the true nonrelativistic value. Hence comparisons of DFT total energies with total energies from other methods cannot be used as an indication of basis set convergence. However, comparison of DFT total energies calculated using different basis sets but the same functional is useful for this purpose. With the exception of the out of plane component of the polarizability tensor, the dipole moment and polarizability components seem to be converging to values in reasonably good agreement with experiment. Since the dipole moment and polarizability can be defined in terms of derivatives of the total energy with respect to an applied electric field, the fact that the LDaxc results for these properties are better than for the total energy is consistent with the well known fact that density-functional calculations often give much better relative than absolute energies.

Figure 1 shows the basis set convergence of the TKSA MD for the $1b_1$ orbital of water. The CI MD of Davidson *et al.* [4] is included only as a reference for the reader's convenience. As seen from Fig. 1, the convergence properties of the MD's generally reflect those observed in Table I for the energy, dipole moment, and components of the polarizability tensor, except that the addition of FIP functions to the basis is more efficacious for the dipole moment and polarizability than for MD's, which is not surprising since these functions were designed for calculating dipole polarizabilities. Nevertheless, since a good description of the large- r region is important for MD's, the FIP's, being diffuse functions, do have a significant effect on the MD when added to the TZP and ANO- basis sets (to give TZP+ and ANO+). However, this effect of the diffuse FIP's on the MD is almost imperceptible for the larger NHF- basis set. Although no attempt was made to go beyond the NHF+ to try to fully saturate the basis, the MD's appear to be reasonably well converged.

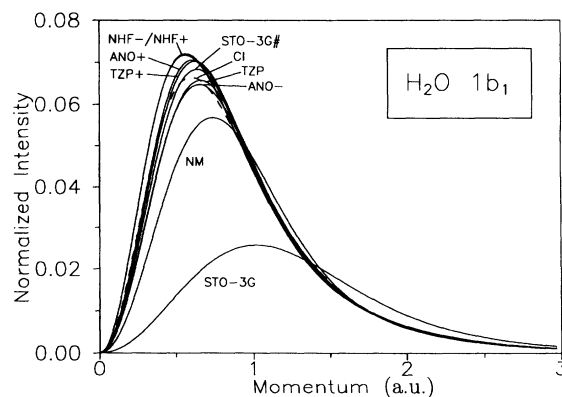


FIG. 1. Effect of basis set on the TKSA MD for the $1b_1$ orbital of H_2O , using the LDaxc functional and the basis sets described in the text. The CI/109CGTO MD of Ref. [4] (dashed curve) is shown for comparison purposes. All MD's have been calculated from orbitals which are normalized to unity.

Judging from the convergence of the total energy, dipole moment, polarizabilities, and MD's, the ANO+ basis seems to be of good quality, while being only moderately large, and offering a uniform level of description for the different molecules studied. This level of convergence should be quite adequate for the purpose of the present study, which is to investigate the viability of using KS orbitals to approximate Dyson orbitals for calculating MD's. The ANO+ basis set will therefore be used throughout the rest of this study.

It is worth noting that the STO-3G# basis gives remarkably good MD's for such a small basis set. This is typical for this basis. This is because the STO-3G# basis set was created from the overly small STO-3G basis set by adding diffuse functions specifically designed to increase the ability of this basis set to describe the large- r behavior, which is of primary importance for calculating MD's [34]. Since the resultant basis set is still quite small, it provides an efficient approximate method for the cal-

ulation of MD's for large molecules. On the other hand, Table I shows that the same cannot be said for the dipole moment and polarizability, for which a good description in the small- r as well as the large- r region is needed.

One further step is necessary in order to compare theoretical MD's with experiment, namely, the finite momentum (i.e., angular) resolution of the experimental apparatus must be taken into account, either by incorporating the experimental resolution into the theoretical MD's or by removing the finite resolution from the experimental XMP's by some sort of deconvolution procedure. At the present time, given the statistics of a typical EMS experiment, the latter is impractical. Hence, when comparing theory with experiment, we take the former approach and use the procedure given in Ref. [108] to resolution-fold MD's in order to compare with XMP's. In addition, since absolute-intensity XMP's are not yet obtainable from EMS experiments, the XMP's for different orbitals in the same molecule are normalized only relative to one

TABLE I. Basis-set dependence of the total energy, dipole moment, and principal components of the dipole polarizability of H₂O. The molecule is oriented in the (x,z) plane with its dipole aligned along the z axis. The basis sets are listed in order of decreasing total energy. The basis sets used in the deMon calculations are described in the text; those used in the MELD and HONDO8 calculations are described in the appropriate references. Results for the polarizability are not available for the MELD calculations.

Method/Basis set	Size ^a	Dipole moment (a.u.)	Polarizability (a.u.)			Total energy (a.u.)
			α_{xz}	α_{yy}	α_{zz}	
deMon calculations ^b						
LDAXc/STO-3G	7	0.6807	4.778	0.040	2.163	-74.7331
LDAXc/STO-3G#	10	0.9533	4.644	0.182	3.047	-74.8820
LDAXc/NM	36	0.8104	7.989	4.634	6.498	-75.8868
LDAXc/TZP	29	0.8532	7.895	4.057	6.653	-75.8996
LDAXc/TZP+	42	0.7455	10.290	9.942	10.114	-75.9031
LDAXc/ANO-	61	0.7489	9.327	7.068	8.703	-75.9113
LDAXc/ANO+	73	0.7334	10.430	9.890	10.234	-75.9127
LDAXc/NHF-	92	0.7597	9.508	9.533	9.032	-75.9129
LDAXc/NHF+	104	0.7366	10.434	10.574	10.391	-75.9132
HONDO8 calculations ^c						
HF/[10s7p4d/7s4p]	93	0.780	9.16	7.91	8.46	-76.0654
MELD calculations ^d						
HF/99CGTO	99	0.7893				-76.0669
HF/109CGTO	109	0.7891				-76.0671
HF/140CGTO	140	0.7794				-76.0673
CI/99CGTO	99	0.7439				-76.3736
CI/109CGTO	109	0.7455				-76.3761
CI/140CGTO	140	0.7356				-76.3963
Experimental values						
		0.727 ^e	10.31 ^f	9.55 ^f	9.91 ^f	-76.4396 ^g

^aNumber of contractions of Gaussian-type orbitals.

^bPresent work. The total energy is the "analytic energy" calculated using both charge density and exchange-correlation fitting functions.

^cTaken from Ref. [26].

^dAll MELD calculations are taken from Ref. [3] with the exception of the 109CGTO calculation which is from Ref. [4].

^eReference [118].

^fReference [119].

^gFrom Ref. [3].

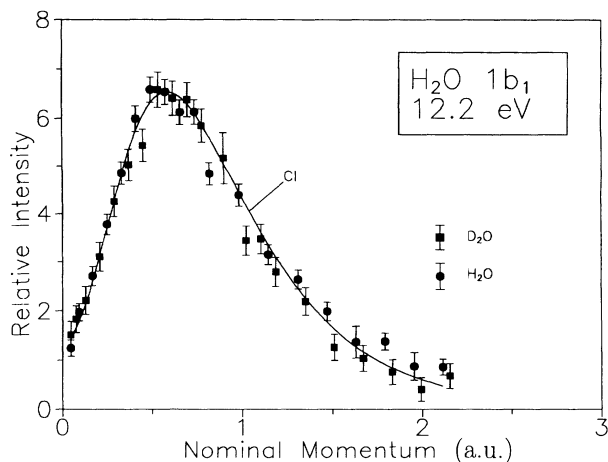


FIG. 2. Comparison of the experimental XMP and resolution-folded CI/109CGTO MD for the $1b_1$ orbital of H_2O . Both the experimental data and CI MD have been taken from Ref. [4], but the resolution-folding of the CI MD has been done according to the prescription given in Ref. [108] for a more appropriate comparison between theory and experiment.

another, but not on an absolute scale. Thus, in order to compare experiment and theory, the arbitrary normalization constant is fixed by scaling the data such that the height of the XMP agrees with the resolution-folded CI MD for one orbital in each molecule.

It is well established that the resolution-folded CI MD's of Davidson *et al.* are in excellent agreement with experiment [3–13,108]. This is illustrated in Fig. 2 for the $1b_1$ orbital of H_2O . Thus these high-quality CI MD's can be used as a reference against which to judge the MD's obtained from DFT approximations to Dyson orbitals.

IV. RESULTS AND DISCUSSION

This section presents the results of our assessment of the target Kohn-Sham approximation (TKSA) for the calculation of MD's, within the LDA, for 18 orbitals in six small molecules and atoms where high-quality HF and CI calculations as well as experimental data are available for comparison. The experimental results used here are those of Brion *et al.* at the University of British Columbia, while the CI MD's are those of Davidson *et al.* at the University of Indiana. The excellent agreement found between these high-quality CI MD's and the experimental results [3–5,9,10,12] allows us to use these CI MD's as a standard against which to assess our DFT approximations. We also consider, in Sec. IV B, two interesting *ad hoc* approximations. In the final subsection we return to the TKSA and take a preliminary look at the effect of different approximate functionals.

The calculation of spectroscopic factors requires a perturbative treatment going beyond the basic KS or HF calculation [see Eq. (2.25)] and is thus computationally more involved. And for purposes of using MD's to assign peaks in EMS spectra, theoretically calculated spectro-

scopic factors are not necessary. Thus we do not calculate spectroscopic factors, but make the comparisons in terms of the renormalized Dyson orbitals $\tilde{\psi}_I^{(i)}$ which have the spectroscopic factors divided out [Eq. (2.26)]. In the THFA or TKSA, $\tilde{\psi}_I^{(i)}$ is just the (canonical) HF or KS orbital ϕ_i [Eq. (2.27)], while the experimentally determined [via Eq. (2.31)] and CI spectroscopic factors are divided out of their respective XMP's or MD's.

In view of the resolution folding and height scaling (described in the previous section) involved in comparing theory with experiment, and the size of the error bars on the experimental data, the cleanest test of the DFT orbital MD's for these small molecules is in comparison with the CI MD's. Comparison with the experimental results is, of course, also important, since the adequacy of the DFT results for use in EMS peak assignments is of primary concern.

A. Target Kohn-Sham approximation in the LDA

A practical investigation of the TKSA necessarily involves the use of an approximate exchange-correlation functional. The present study focuses primarily on the TKSA in the local density approximation (LDA), though the effect of the functional is investigated for H_2O in Sec. IV C. The present subsection deals with the results using the LDAXc functional.

In order to test the quality of the KS orbital MD's obtained from the TKSA (in the LDA), six small molecules, HF, H_2O , NH_3 , CH_4 , C_2H_2 , and Ne, were chosen whose EMS has been well studied both experimentally and theoretically [3–5,9,10,12,13,108], and calculations of the MD's were carried out for all the valence orbitals. H_2O is a particularly interesting test molecule because it is more difficult to obtain a quantitative description of the MD for the HOMO, and to a lesser extent the $3a_1$ orbital, than for the outer valence orbitals of many other molecules.

Figures 3 and 4 show the calculated momentum distributions (MD's) for all the valence orbitals of water and acetylene, respectively. In addition to the KS orbital MD's, these figures contain the results from the KSKH and TOM orbital approximations which will be discussed in the next subsection. Looking now at the KS results, it is immediately evident that the positions and shapes of the KS, HF, and CI MD's are all very similar, the primary difference between them being in the peak heights. This is also the case for the other molecules studied, so for the remaining molecules only the peak heights and positions are reported here. The results are shown in Fig. 5 and Table II.

It is evident from Figs. 3–5 and Table II that the overall quality of the TKSA in the LDA is quite similar to that of the THFA for the orbital MD's of these molecules. For some orbitals the KS MD's are a little better than the HF, while for others the HF is a little better, and for many orbitals the magnitude of the error in the KS peak height parallels that for the HF, being larger when correlation is more important. For both the KS and HF

MD's, the largest error in the peak height occurs for the $2\sigma_g$ orbital of acetylene. The errors in the heights of the KS MD's, compared to CI, range from 1% to 6%, with the exception of the $2\sigma_g$ orbital of acetylene with an error of 17% and the $2a_1$ orbital of CH_4 with an error of only 0.4%. In comparison, the peak height errors in the HF MD's are in the range 2% to 11%, except for four orbitals ($\text{CH}_4 1t_2$, $\text{NH}_3 2a_1$ and $1e$, and $\text{H}_2\text{O } 1b_2$) having errors of 0.3% or less. The average error of 4.6% in the peak heights for all the orbitals is the same for the KS and HF MD's. The errors, again relative to the CI, in the positions of the peaks, i.e., in the value of the momentum for which the MD has its maximum, are often less than the estimated uncertainty in the determination of this value and the average error (excluding those orbitals for which symmetry constrains the maximum to occur at zero momentum) is 1.4% and 1.9% for KS and HF, respectively.

It is interesting to note that, while the magnitude of the errors in the KS and HF MD's are quite similar, KS and HF results are usually off in *opposite directions*. The

maximum of the MD is shifted, if at all, to higher momentum in the HF and to lower momentum in the KS MD's. Out of the 18 orbitals treated here, the height of the MD from the KS is greater than that from the CI calculation for 14 orbitals, and the HF MD height is less than the CI MD height for 15 orbitals. (In only one case is the height from the KS less than that from the HF calculation.) While both KS and HF orbitals approximate Dyson orbitals, and apparently about equally well for the MD's, they do so in different ways.

Of course the quantitative aspects of the errors in the TKSA vs THFA would be expected to depend on the basis sets used in the respective calculations. For example, the peak height errors might be somewhat larger in the "LDA limit" than those reported here. However, in view of the level of convergence of the MD's shown in Fig. 1, the basic conclusion that the TKSA (in the LDA) and the THFA are of roughly comparable quality for MD's, seems unlikely to be altered by further improvements in the basis set.

Figure 6 shows the resolution-folded KS, HF, and CI

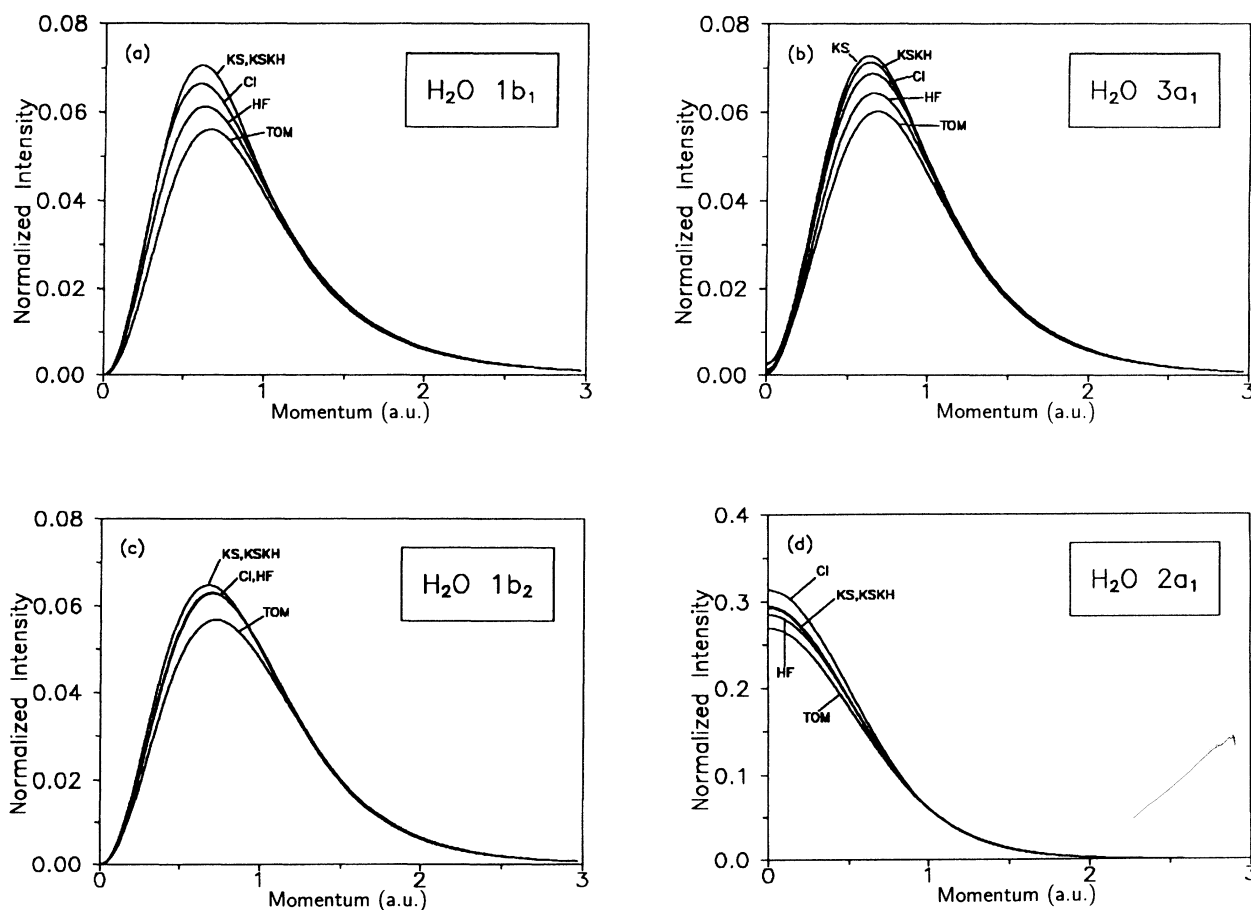


FIG. 3. Comparison of several DFT approximations for MD's with target Hartree-Fock and CI MD's, for the valence orbitals of H_2O . The DFT calculations used the LDAxc functional and the ANO+ basis set. The CI calculations are the 109CGTO basis set calculations of Ref. [4], while the HF calculations are those of Ref. [3], using the 99CGTO basis set, except for the $2a_1$ orbital, where only the 84CGTO calculation of Ref. [117] was available (at the HF level the 84CGTO, 99CGTO, and 109CGTO MD's are indistinguishable from one another). The curve labels are target Hartree-Fock approximation (HF), configuration interaction (CI), target Kohn-Sham approximation (KS), Kohn-Sham Koopmans' hole (KSKH), and transition orbital method (TOM).

MD's in comparison with the experimental data for H_2O . The arbitrary normalization of the experimental XMP's has been fixed by scaling the data such that the height of the peak matches the CI result for the $1b_1$ orbital. Since practical applications of the DFT MD's where no CI calculation is available would require a similar scaling, except that the data would be normalized to a KS orbital, a fourth curve has been included in which the KS MD's have been scaled (by a factor of 0.94) such that the $1b_1$ orbital peak height matches that of the CI calculation (and thus the experiment). While such rescaled MD's are appropriate from the point of view of practical applications, they do not give an accurate indication of the relative quality of the different theoretical models since the most pronounced difference between the theoretical MD's is in the peak heights. The TKSA MD's in Fig. 6 are certainly of good quality from the point of view of applications to EMS, and the same is true for the other molecules we have studied.

While both the shape and the height of the orbital MD are sensitive to the large- r behavior of the orbital, this relationship is stronger for the shapes than for the heights [34]. Thus a tendency to give good MD *shapes* may be an

indication of the quality of the large- r behavior of the KS orbitals. This would be consistent with the previously observed [26] good quality of DFT dipole moments, polarizabilities, and hyperpolarizabilities, since these properties also depend upon a good description in the large- r region. Although it is well known that the presently available functionals do not give the correct asymptotic behavior of the exchange-correlation potential, Umrigar and Gonze's calculations of the exact exchange-correlation potential [109,110] for He and Ne suggest that, for physically relevant large distances, the approximate potentials are off by an almost constant shift, whereas the behavior close to the nucleus is more problematic.

B. *Ad hoc* DFT approximations for Dyson orbitals

Two interesting but *ad hoc* approximations for Dyson orbitals were presented at the end of Sec. IID. The TOM approximation consists of using the transition orbital obtained in Slater's transition state method, while the KSKH approximation involves carrying out a KS DFT calculation on the daughter ion in the restricted space of

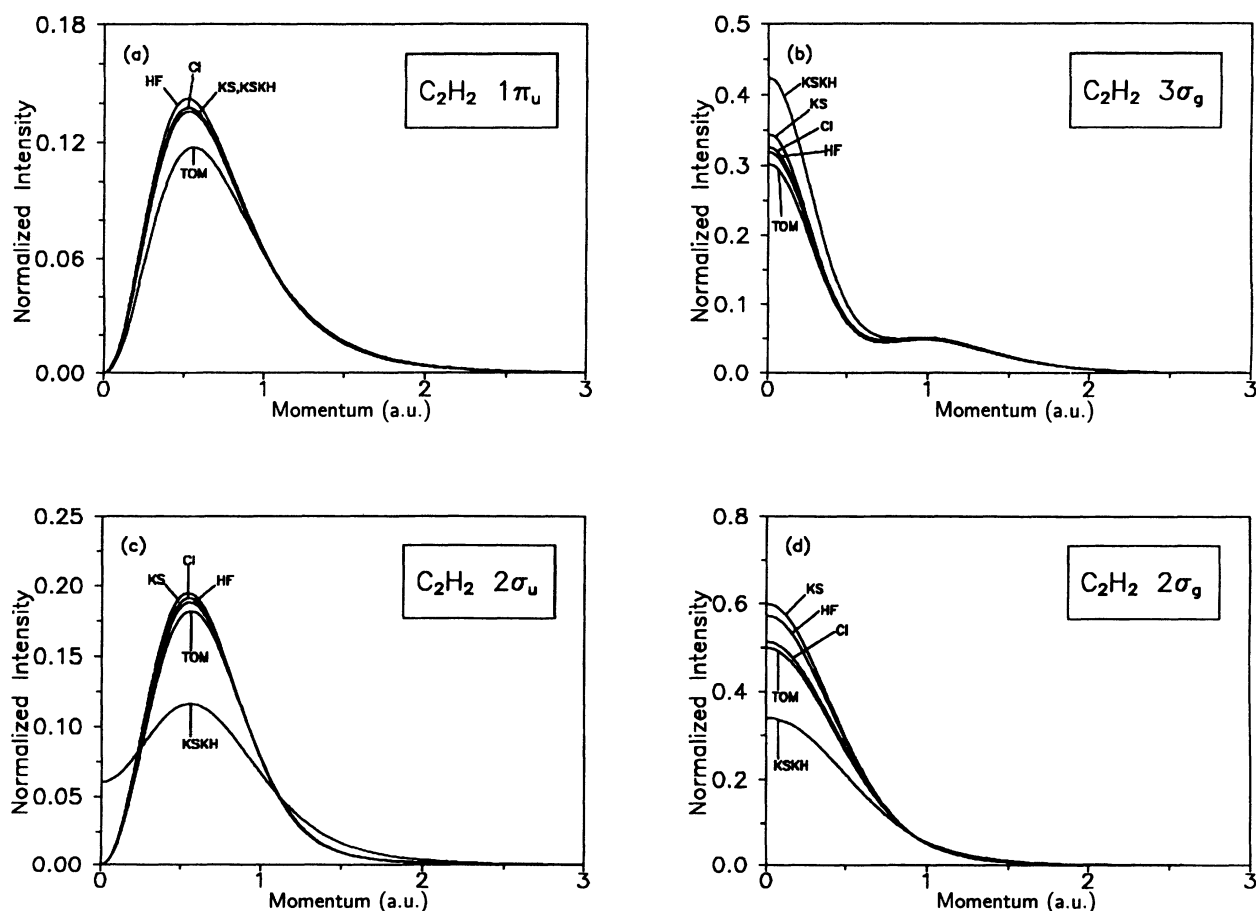


FIG. 4. Comparison of several DFT approximations for MD's with target Hartree-Fock and CI MD's, for the valence orbitals of C_2H_2 . The DFT calculations used the LDAxc functional and the ANO+ basis set. The Hartree-Fock and CI calculations are the 186CGTO calculations from [12]. The curve labels are target Hartree-Fock approximation (HF), configuration interaction (CI), target Kohn-Sham approximation (KS), Kohn-Sham Koopmans' hole (KSKH), and transition orbital method (TOM).

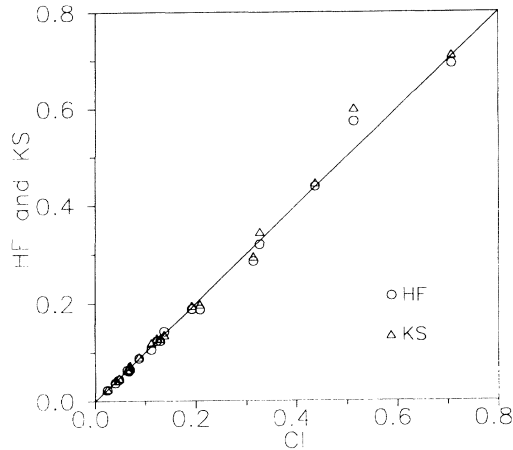


FIG. 5. Correlation plot of the MD peak heights obtained in the target Kohn-Sham approximation (KS) and in the target Hartree-Fock approximation (HF) with configuration interaction (CI). Values are from Table II.

TABLE II. Absolute peak heights and positions of the maxima of MD's for the valence orbitals of all six molecules in the present study. Positions should be considered accurate to only ± 0.025 a.u. and heights to within 1%. KS/LDAxc: Target Kohn-Sham approximation using the LDAxc functional and ANO+ basis set. HF: Target Hartree-Fock approximation. CI: Multireference singles and doubles configuration-interaction calculation. Positions and heights are given in atomic units. The HF and CI calculations are taken from the following references: CH₄ [9], NH₃ [5], HF [10], Ne [13], and C₂H₂ [12]. For H₂O, the CI calculations are the 109CGTO basis-set calculations of Ref. [4] while the HF calculations are those of Ref. [117] using the 99CGTO basis set, except for the 2a₁ orbital, where only the 84CGTO calculation of Ref. [117] was available (at the HF level the 84CGTO, 99CGTO, and 109CGTO MD's are indistinguishable from one another).

Orbital	KS/LDAxc		HF		CI	
	Position	Height	Position	Height	Position	Height
			CH ₄			
2a ₁	0.0	0.7100	0.0	0.6923	0.0	0.7074
1t ₂	0.567	0.1288	0.600	0.1228	0.567	0.1231
			NH ₃			
2a ₁	0.0	0.4451	0.0	0.4381	0.0	0.4370
1e	0.633	0.09037	0.633	0.08704	0.633	0.08709
3a ₁	0.533	0.1185	0.533	0.1049	0.533	0.1121
			H ₂ O			
2a ₁	0.0	0.2947	0.0	0.2851	0.0	0.3137
1b ₂	0.667	0.06473	0.700	0.06288	0.700	0.06307
3a ₁	0.633	0.07277	0.650	0.06438	0.633	0.06877
1b ₁	0.600	0.07061	0.650	0.06113	0.600	0.06643
			HF			
2σ	0.0	0.1976	0.0	0.1872	0.0	0.2077
3σ	0.733	0.04716	0.766	0.04373	0.733	0.04650
1π	0.700	0.04239	0.733	0.03714	0.733	0.03930
			Ne			
2s	0.0	0.1277	0.0	0.1227	0.0	0.1297
2p	0.833	0.02443	0.850	0.02256	0.850	0.02355
			C ₂ H ₂			
2σ _g	0.0	0.5999	0.0	0.5729	0.0	0.5136
2σ _u	0.533	0.1950	0.550	0.1883	0.550	0.1915
3σ _g	0.0	0.3447	0.0	0.3195	0.0	0.3265
1π _u	0.533	0.1359	0.525	0.1425	0.525	0.1379

the parent occupied molecular orbitals to obtain the orbital for the hole and using this "KSKH" orbital. Just as for the canonical KS orbitals, both the KSKH and TOM orbitals are used to approximate Dyson orbitals *via the target approximation*. The results for H₂O and acetylene, using the LDAxc functional, are shown in Figs. 3 and 4, respectively.

Consider first the KSKH approximation. For H₂O, the 1b₁ and 1b₂ orbitals are lone symmetry states, so these KSKH orbitals should be identical to the canonical KS orbitals. This was indeed found to be the case in our calculations, which constitutes a useful check. Mixing of the three parent a₁ states is allowed by symmetry, so the KSKH orbitals can differ from the canonical KS orbitals for these states. Nevertheless, Fig. 3 shows that the 3a₁ and 2a₁ KSKH orbital MD's are quite similar to the canonical KS orbital MD's. For acetylene (Fig. 4), the 1π_u orbital is a lone symmetry state, and the KSKH and canonical KS orbitals were again found to be iden-

TABLE III. Symmetry breaking in DFT calculations on excited states of C_2H_2 as indicated by the nonzero dipole moment. The dipole moment is that of the daughter ion formed by removing an electron (half an electron in the case of the transition orbital method) from the orbital indicated. All calculations were performed with the origin at the center of inversion symmetry for the molecule.

Orbital	Transition orbital method	Dipole moment (a.u.)	
		Kohn-Sham	Koopmans' hole orbitals
$1\pi_u$	0.0000	0.0000	0.0000
$3\sigma_g$	0.0021	4.2457	4.2457
$2\sigma_u$	0.6884	3.2158	3.2158
$2\sigma_g$	0.0002	0.0000	0.0000

tical. But for the other states the KSKH and canonical KS orbital MD's look quite different. However, except for the case of ionization from the HOMO, these KSKH calculations involve excited states of the ion. Unfortunately, significant symmetry breaking, i.e., obtaining orbitals which do not belong to the irreducible representations of the symmetry group for the molecule, sometimes occurs in KS DFT calculations for excited state config-

urations, and our KSKH calculations are no exception. This is readily apparent in the KSKH orbital MD for the $2\sigma_u$ orbital of acetylene which should vanish at zero momentum, by symmetry, but which does not. Symmetry breaking is apparent for the $3\sigma_g$, as well as the $2\sigma_u$, KSKH orbital, from Table III, which shows the dipole moment, in center of mass coordinates, of the daughter ion. No symmetry breaking is evident for the $2\sigma_g$ or-

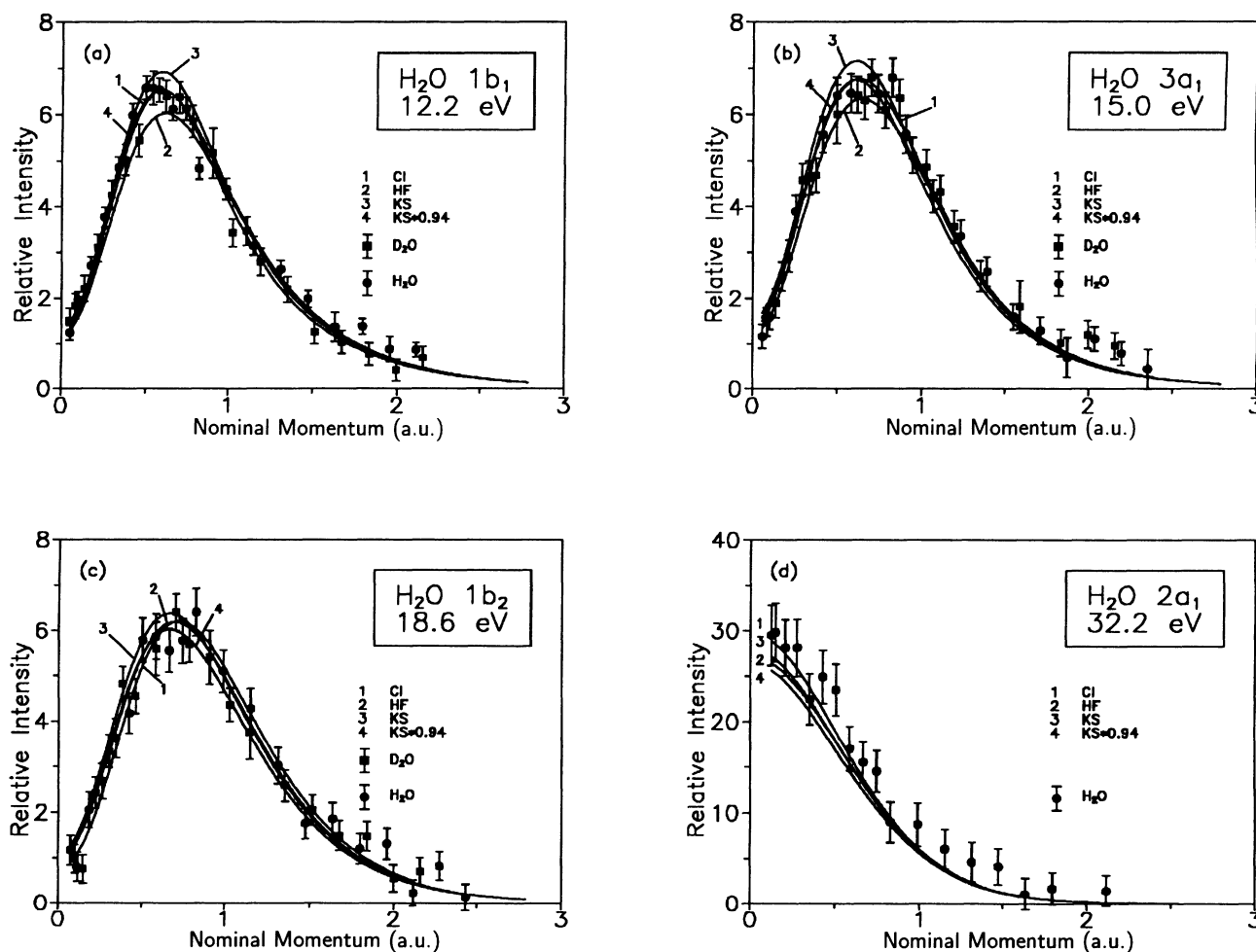


FIG. 6. Comparison of target Kohn-Sham approximation (KS), target Hartree-Fock approximation (HF), and CI MD's with experimental XMP's for the valence orbitals of H_2O . The theoretical MD's are those of Fig. 3, but here they have been resolution folded according to the prescription given in Ref. [108] in order to compare with experiment. Two KS MD's are shown for each orbital. The first retains the absolute intensity from the original calculation, while the second is multiplied by 0.94 (for all orbitals) so that the heights of the CI and KS MD's for the $1b_1$ orbital match (see text).

bital, though we view this KSKH orbital with caution. The KSKH orbital MD for this orbital differs markedly from the canonical KS orbital MD. Considering all the orbitals of both molecules, the question remains open as to how much of the observed difference between the KSKH and canonical KS orbitals is attributable to problems with the excited state DFT calculations and how much is a real effect. It is clear, however, that, due to the vagaries of excited state DFT calculations, the KSKH approach is not reliable enough to be useful as an *ad hoc* DFT approximation to Dyson orbitals, and the results do not appear to be particularly better than those for the canonical KS orbitals anyway.

The TOM also involves DFT calculations using excited state configurations, and some symmetry breaking in the TOM calculations on acetylene is apparent from the dipole moments (Table III), though to a much lesser extent than in the KSKH calculations. Nevertheless, the transition state method often provides excellent estimates of ionization potentials [20,93,111]. Recall that the motivation for considering the TOM here is that the MD is sensitive to the asymptotic behavior of the orbital, which is in turn related to its eigenvalue. Thus one might think to improve the MD's by improving the orbital energies. For all the valence orbitals of H_2O and C_2H_2 (Figs. 3 and 4) the height of the TOM orbital MD is less than the height of the corresponding KS orbital MD. A rough qualitative explanation of why this is so can be given in terms of the ionization potentials, since this is the primary difference between the KS and TOM approximations. As illustrated in Table IV, while the transition state method eigenvalue is a good approximation to the negative of the orbital ionization potential, the negative of the KS orbital energy gives an ionization potential which is substantially too low. A higher ionization potential would generally be expected to correspond to a more contracted orbital in position space [as is consistent with Eq. (2.6), for neutrals], which leads to a loss of MD amplitude at low momentum, by the well known Fourier correspondence between position and momentum space distributions [34]. Although the KS orbital MD's

do tend to be too high, this "correction" is too extreme. In all but one of the eight orbitals in Figs. 3 and 4, the TOM MD is *further* from the CI MD than is the KS MD, and there is a marked disagreement between the TOM and CI MD's for the $1\pi_u$ orbital of acetylene and all the valence orbitals of water. These results for the TOM MD's serve to illustrate that, even for the purpose of calculating MD's, a property which is particularly sensitive to the large- r behavior of the orbital and hence to its eigenvalue, approximating the Dyson orbital is not synonymous with approximating its eigenvalue.

C. Effect of the functional

The results in the previous two subsections, on the TKSA and on the *ad hoc* KSKH and TOM approximations, are all at the level of the local density approximation, LDAxc (LDA including both exchange and correlation). The present subsection returns to the TKSA and gives a preliminary investigation of the effect of the functional, for H_2O . We consider the effect of gradient corrections, as well as the separate contributions of the exchange and correlation functionals.

Among the well known problems with the local density approximation are self-interaction errors, overbinding of molecules, and an exchange-correlation (xc) potential which falls off too rapidly, asymptotically. One might expect that this last point would be important for MD's. The physical effect of an xc potential which falls off too rapidly is that an electron in the large- r region experiences the full non-self-interaction-corrected Hartree potential for N electrons instead of the correct potential for $(N-1)$ electrons. This makes the electron less bound than it should be, its position space orbital too diffuse, and the corresponding MD have too large an amplitude at small p . This is consistent with the TKSA results reported in Sec. IV A.

Given the sensitivity of MD's to the large- r region, we have chosen to use the 1988 exchange correction of

TABLE IV. Comparison of the negative of Kohn-Sham orbital energies at full (KS orbital energy) and half (transition state method) occupancy with experimental ionization potentials, for C_2H_2 and H_2O , using the LDAxc functional and the ANO+ basis set. The experimental values are taken from Ref. [12] for C_2H_2 , and from Ref. [120] for H_2O . The ionization potential "of the $2a_1$ orbital" of H_2O is not well defined, due to the severe breakdown of the one-electron picture in this region of the binding-energy spectrum.

Orbital	KS orbital energy	Ionization potentials (eV)		Experiment
		C_2H_2	Transition state method	
$1\pi_u$	7.31		11.70	11.40
$3\sigma_g$	12.23		16.74	16.7
$2\sigma_u$	13.99		18.48	18.9
$2\sigma_g$	18.48		23.69	23.5
		H_2O		
$1b_1$	7.36		13.13	12.6
$3a_1$	9.40		15.23	14.7
$1b_2$	13.33		19.27	18.6
$2a_1$	25.23		31.65	

Becke [102]. This was combined with the 1986 correlation correction of Perdew [103]. The Becke functional gives the correct asymptotic behavior of the exchange energy density $\epsilon_x(\mathbf{r})$, which is expected to improve the asymptotic behavior of the exchange potential $v_x(\mathbf{r})$. Nevertheless, it should be noted that the B88x potential still does not have the correct asymptotic form. Figure 7 shows the TKSA MD's for the valence orbitals of water as well as the corresponding THFA and CI MD's. The KS orbitals have been calculated using the LDAx and B88x exchange-only functionals and the LDAxc and B88x+P86c exchange-correlation functionals. The effect of the B88x and P86c gradient corrections on these MD's is to lower the peak heights slightly. This constitutes an improvement for the three outer valence orbitals, but not for the inner valence orbital where the LDA (x and xc) MD's were already below the CI.

As mentioned in Sec. IID, the exact exchange-only KS orbitals have been calculated for atoms and have been found to be remarkably similar to HF orbitals. This

would lead one to expect that the exchange-only TKSA should give very similar MD's to the THFA MD's, if the functional were exact. However the difference between the LDAx TKSA MD's and the THFA MD's shown in Fig. 7 is dramatic. This difference is probably primarily due to deficiencies in the LDAx functional. Nevertheless, in the absence of MD's calculated from the exact KS orbitals, we cannot rule out the possibility that the difference might be real and not an artifact of the functional used. The B88x functional is expected to improve the description of the asymptotic behavior of the KS exchange potential. However, this gradient correction moves the MD's for the exchange-only KS orbitals only a little closer to the THFA MD's.

An interesting thing about the curves in Fig. 7 is the effect of including correlation in the functional. This acts to *reduce* the height of the TKSA MD's, whereas the CI MD's for these orbitals have a *larger* amplitude than do the corresponding THFA MD's. Since a more diffuse (contracted) orbital generally corresponds to a

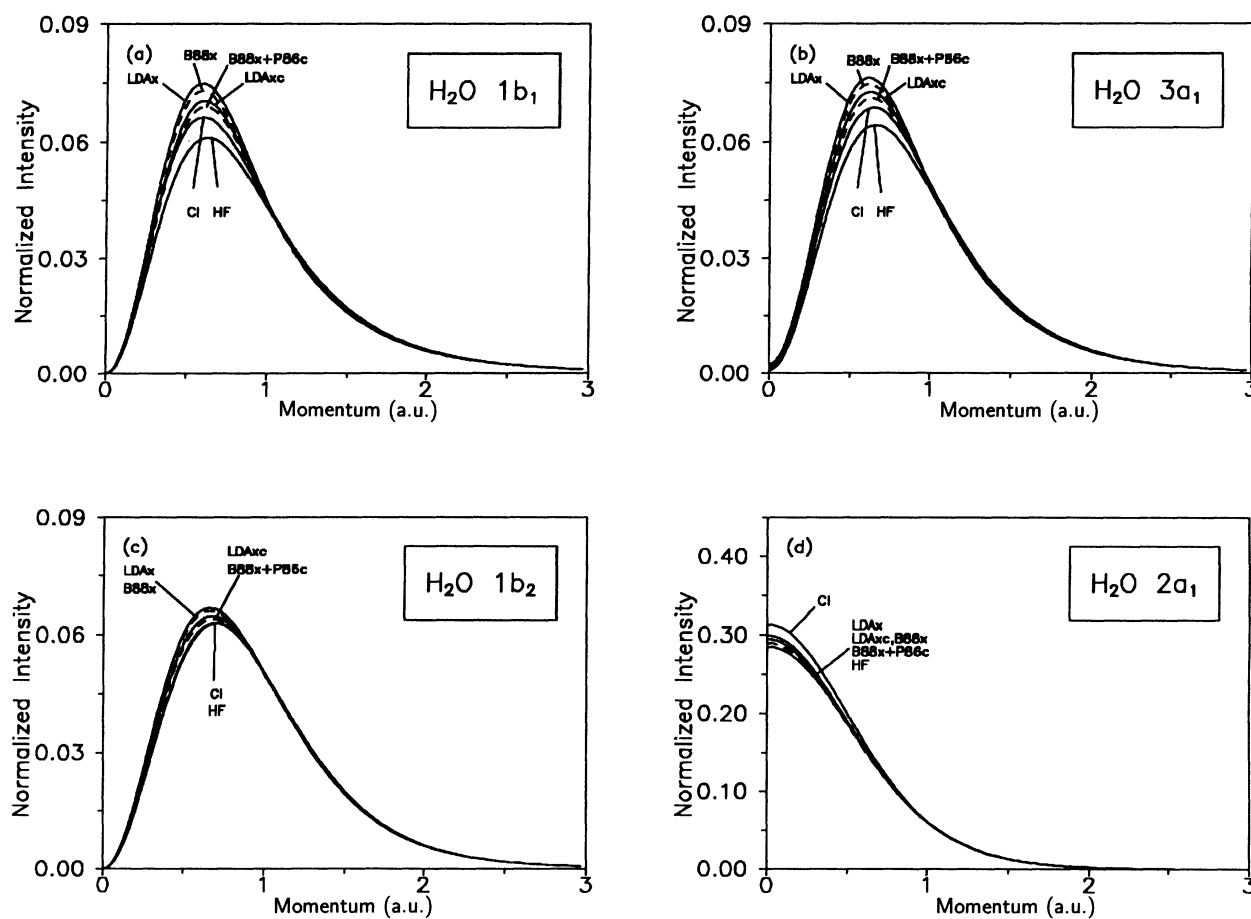


FIG. 7. Effect of the exchange-correlation functional on the target Kohn-Sham approximation MD's, for the valence orbitals of water. The curve labels are exchange-only local density approximation (LDAx); exchange-correlation local density approximation (LDAxc); exchange-only functional using Becke's 1988 gradient correction (B88x); exchange-correlation functional using Becke's 1988 gradient correction for exchange and Perdew's 1986 gradient correction for correlation (B88x+P86c); target Hartree-Fock approximation (HF); configuration interaction (CI). Dashed curves are used for MD's calculated with gradient-corrected functionals. The density-functional calculations use the ANO+ basis set. The HF and CI calculations, taken from Refs. [3,4,117] are those shown in Fig. 3.

higher (lower) amplitude MD, the correlation functionals used here appear to result in a contraction of the outer orbitals and hence of the overall charge density, while the addition of electron correlation to the Hartree-Fock calculation acts to make the valence Dyson orbitals, and hence the overall charge density, more diffuse. This is an indication that electron correlation is being treated differently in DFT than in conventional *ab initio* electronic structure methods.

This same effect has been previously observed [112] for dipole polarizabilities, another property which is sensitive to the large- r behavior of the charge density. Table V shows the experimental and Hartree-Fock dipole polarizabilities of water as well as polarizabilities calculated using the same basis sets and density functionals used elsewhere in the present study. It is evident that the exchange-only calculations overestimate the diffuseness and hence the polarizabilities while the exchange-correlation density functionals give much more reasonable results.

An explanation was proposed in Ref. [112] where it was noted that correlation manifests itself through two competing effects. On the one hand, an admixture of excited state configurations in the many-electron wave function tends to make the electron density more diffuse, hence increasing the polarizability. On the other hand, electron correlation enhances the ability of the electrons to avoid each other, hence minimizing the effects of electron repulsions and leading to a more contracted charge density. Present density functionals appear to emphasize the latter effect for MD's and polarizabilities, although the former effect should apparently be the dominant one

for these properties.

This picture seems physically reasonable, providing we refine it by recognizing that which one of these two effects of correlation dominates may vary from one region of space to another. This is easiest to see for atoms. Since electron correlation lowers the total electronic energy, by the virial theorem, it must also increase the kinetic energy. One way for this to happen is for the electrons to move closer to the nucleus in the energetically important core region. At the same time, this contraction of the core increases the screening of the nuclear charge, thereby allowing the outer, valence parts of the charge density to expand. This general picture is consistent with findings on the exact correlation potential for two electron atoms [110,113]. Umrigar and Gonze [110] have compared this exact correlation potential with correlation potentials calculated from the LDA and various state-of-the-art functionals and find that the correlation potentials from the approximate functionals have on average the wrong sign in comparison with the exact result. However, this tends to counteract errors in the exchange potential, so the net effect is a cancellation of errors in the exchange and correlation functionals. Thus, in spite of the shortcomings of the correlation functionals, the xc functionals do generally improve upon the exchange-only calculation.

V. CONCLUSIONS

This paper introduces the target Kohn-Sham approximation (TKSA) for use in the analysis of electron-

TABLE V. Effect of exchange-correlation functional on the dipole moments and polarizabilities of H₂O, using the ANO+ basis set. The molecule is oriented in the (x,z) plane with the dipole along the z axis. The notations "x" and "c" refer respectively to the inclusion of exchange and correlation in the functional. HONDOS near-Hartree-Fock-limit results have been included for comparison purposes.

Method	Dipole Moment (a.u.)	Polarizability (a.u.)		
		α_{xx}	α_{yy}	α_{zz}
Local density approximations				
LDAx ^a	0.7204	10.985	10.673	10.906
LDAXc ^b	0.7334	10.430	9.890	10.234
Gradient-corrected functionals				
B88x ^c	0.6997	10.855	10.369	10.661
B88x ^c +P86c ^d	0.7135	10.364	9.779	10.110
Experimental values ^e				
	0.727	10.31	9.55	9.91
HONDOS calculations ^f				
HF	0.7802	9.16	7.91	8.46

^aOriginal $X\alpha = 2/3$ functional of Kohn and Sham [29].

^bAs parametrized by Vosko, Wilk, and Nusair [100].

^cBecke's 1988 gradient correction for exchange [102].

^dPerdew's 1986 gradient correction for correlation [103].

^eSee the footnotes for Table I.

^fTaken from Ref. [26].

momentum-spectroscopy (EMS) experimental momentum profiles (XMP's). Instead of approximating Dyson orbitals as being proportional to canonical Hartree-Fock orbitals as is done in the well known target Hartree-Fock approximation (THFA), the TKSA approximates Dyson orbitals as being proportional to Kohn-Sham density-functional orbitals. Since density-functional calculations are computationally less demanding than Hartree-Fock calculations, the TKSA provides a more efficient way to calculate Dyson orbitals for use in conjunction with EMS. We have discussed the theoretical foundation for this approximation, as well as given an assessment of the quality of the spherically averaged orbital momentum distributions (MD's) thus obtained.

Density-functional theory has developed from two complementary points of view. In Kohn and Sham's formulation of DFT [29], the true total energy is obtained via a functional of the charge density, and a set of orbitals whose charge densities sum to the true total charge density was introduced as a physically fictitious mathematical device to facilitate representation of the kinetic energy. Sham and Kohn [114] noted the differences between the KS and Dyson equations early on in the history of modern DFT. While their discussion focused on the eigenvalues of the equation rather than the orbitals, it did serve to emphasize that solutions of Dyson's equation cannot be calculated *exactly* within the framework of Kohn-Sham DFT even if the exact exchange-correlation functional were known. The other point of view, dating back to Slater [82], and rigorously formulated by Sharp and Horton [30], Talman and Shadwick [31], and Casida [33], consists of finding the variationally best local approximation to Dyson's quasiparticle equation (or equivalently to the HF equation, in the exchange-only case). Here the KS orbitals and orbital energies are naturally seen as *approximations* to the Dyson (or HF) orbitals and orbital energies. The work of Sham and Schlüter [32] on the exact KS exchange-correlation potential shows that (within the linear response approximation to the Sham-Schlüter equation) these two, formally different approaches both lead to the same Kohn-Sham equation.

The present work is based on the second point of view. Although the idea of KS orbitals and orbital energies as approximate Dyson orbitals and orbital energies is often viewed with skepticism due to the poor quality of this approximation for the orbital energies, this by no means implies a corresponding problem with the orbitals. Indeed, our examination of the nature of the localization process, in the Appendix, clarifies why the KS eigenvalues should be shifted even if the orbitals are quite good approximations to the Dyson orbitals. The various theoretical considerations involved in the approximation of Dyson orbitals by Kohn-Sham orbitals, including the introduction of the target Kohn-Sham approximation, were presented in Sec. II.

The rest of the paper has been devoted to investigating the practical utility of the TKSA for the calculation of MD's for use in EMS. This necessarily involves a second approximation, namely, the use of approximate functionals. Results using the local density approximation (LDA) for the Kohn-Sham exchange-correlation functional have

been presented for 18 orbitals in six small molecules and atoms where high quality CI and HF calculations as well as experimental data are available for comparison. The quality of these results for the TKSA is about the same as that of the THFA. It is interesting to note that while the magnitude of the error in the TKSA peak heights and positions is generally similar to that in the THFA, the direction of the error in the TKSA is often opposite to that in the THFA. Both KS and HF orbitals approximate Dyson orbitals, but they do so in different ways.

The effect of using different approximations for the exchange-correlation functional was considered for H₂O. From this it appears that part of the observed difference between the TKSA and the CI MD's may be due to the approximate functionals used rather than to the underlying approximation of Dyson orbitals by KS orbitals via the TKSA. Just how much of the error is due to which of these two approximations is an interesting question whose answer will require the calculation of MD's from exact KS orbitals.

The success of the target Kohn-Sham approximation introduced here leads to much interesting work which remains to be done. Certainly, the calculation of exact exchange-correlation potentials, for molecules as well as for atoms, which would allow assessment of the quality of the TKSA itself, separate from the question of the approximate functional, would be of fundamental interest. Since EMS probes primarily the large-*r* region, calculation of other orbital-dependent (as opposed to total) properties, as well as direct comparison of the Dyson and KS orbitals in the TKSA, would be very useful in evaluating the overall quality of this approximation. This is particularly important since, as has been pointed out above, while the formal considerations [33] make it clear that the KS orbitals are approximations to Dyson orbitals, there is no *a priori* statement as to how good an approximation this is. For the same reason, the extension of this study to a larger number of molecules, and especially to molecules whose MD's have more complicated shapes, is essential to obtaining an accurate picture both of the overall quality of the TKSA and of its utility for EMS. Work in this direction has already been undertaken by Brion *et al.* at the University of British Columbia, and will be forthcoming shortly [115,116]. And, of course, from a practical point of view, a more extensive investigation of the relative merits of various approximate functionals for calculating MD's would also be useful for EMS.

As the energy resolution and signal to noise ratio of EMS experiments improves, EMS is able to handle larger molecules with increasing accuracy. However, the analysis of these experiments places more severe demands upon the efficiency of the theoretical models. One of the primary advantages of EMS over photoelectron spectroscopy is the ability to assign binding-energy spectra on the basis of comparisons between experimental momentum profiles (XMP's) and calculated spherically averaged orbital momentum distributions (MD's). Of course this advantage can only be realized for molecules where the theoretical calculations can be done. The quality of the MD's obtained in the target Hartree-Fock approximation has proven to be generally adequate for this pur-

pose. Unfortunately, however, the HF calculations have become the limiting factor in determining the size of the molecules whose MD's are feasible to calculate routinely for use with EMS. Since DFT is computationally less demanding than HF calculations, the present finding that the quality of the MD's in the target Kohn-Sham approximation is comparable to that of the THFA MD's is of considerable practical utility for EMS.

ACKNOWLEDGMENTS

We are grateful to Ernest R. Davidson and co-workers for their high-quality HF and CI calculations and to the University of British Columbia EMS group for experimental data. D.P.C. and P.K.J.D. acknowledge financial support from the National Science and Research Council (NSERC) of Canada. M.E.C. and D.R.S. acknowledge financial support from the Canadian Centre of Excellence in Molecular and Interfacial Dynamics. P.K.J.D. would like to thank Alain St.-Amant for help programming the KSKH method, and M.E.C. would like to thank Kim Casida for many helpful discussions.

APPENDIX: ORBITAL ENERGY SHIFT

The purpose of this Appendix is to discuss in more detail why the orbital energies from the Kohn-Sham equation and ionization potentials from Dyson's equation should differ even if the Kohn-Sham orbitals are good approximations to renormalized Dyson orbitals. To this end, let us start by assuming that the target Kohn-Sham approximation (analogous to the target Hartree-Fock approximation), Eq. (2.27), holds. That is,

$$\psi_I(1) \approx \sqrt{S_I^{(i)}} \phi_i(1), \quad (\text{A1})$$

where ϕ_i is a Kohn-Sham orbital. In this approximation, Dyson's equation (2.7) becomes

$$\left[\hat{h}_H + \hat{\Sigma}_{\text{xc}}(\omega_I^{(i)}) \right] \phi_i(1) \approx \omega_I^{(i)} \phi_i(1). \quad (\text{A2})$$

Subtracting this from the KS equation (2.34) gives a closed expression for the xc potential,

$$v_{\text{xc}}(1) \approx \frac{\hat{\Sigma}_{\text{xc}}(\omega_I^{(i)}) \phi_i(1)}{\phi_i(1)} + (\epsilon_i - \omega_I^{(i)}), \quad (\text{A3})$$

in the target KS approximation. The first term on the right-hand side (RHS) is analogous to Slater's orbital-dependent localization procedure [82] for the Hartree-Fock exchange operator and determines v_{xc} up to an orbital-dependent additive constant. [That it is only an additive constant which is undetermined is evident

from the fact that the second term on the RHS is a (possibly orbital-dependent) constant, while the LHS is orbital independent.] Hence the difference between the KS and Dyson orbital energies provides the orbital-dependent constant shift which is needed to yield an orbital-independent v_{xc} . This orbital-dependent shift can also be regarded as a change of energy zero needed to make the RHS of Eq. (A3) go to zero asymptotically. Since the KS and Dyson HOMO orbital energies are equal when the energy zero is chosen such that v_{xc} goes to zero asymptotically, the differences between the KS and Dyson orbital energies must shift the energy zeros of the other orbital-dependent localizations of the self-energy so that all the resultant potentials go to zero asymptotically.

Of course this argument is strictly correct only if the target Kohn-Sham approximation holds exactly. Since it is approximate, the expression (A3) for v_{xc} should be expected to contain some residual orbital dependence. This can be removed by an orbital averaging procedure, as was done by Slater [82] in the exchange-only case. Left multiplying Eq. (A3) by $S_I^{(i)} |\phi_i(1)|^2$ and summing over all orbitals i and final states I , using the relations (2.31) and (2.33), gives

$$v_{\text{xc}}(1) \approx \frac{\sum_i \phi_i^*(1) \left[\sum_I S_I^{(i)} \hat{\Sigma}_{\text{xc}}(\omega_I^{(i)}) \right] \phi_i(1)}{\rho(1)} + \frac{\sum_i |\phi_i(1)|^2 \left(\epsilon_i - \sum_I S_I^{(i)} \omega_I^{(i)} \right)}{\rho(1)} \quad (\text{A4})$$

upon division by $\rho(1)$. It is interesting to note that in the quasiparticle approximation (as defined in Ref. [33]), where $S_I^{(i)} = 1$ and there is only one state I corresponding to each orbital i , this becomes

$$v_{\text{xc}}(1) \approx \frac{\sum_i \phi_i^*(1) \hat{\Sigma}_{\text{xc}}(\omega_I^{(i)}) \phi_i(1)}{\rho(1)} + \frac{\sum_i |\phi_i(1)|^2 (\epsilon_i - \omega_I^{(i)})}{\rho(1)}, \quad (\text{A5})$$

which is the same equation that was derived in Ref. [33] in a different way, starting from the OEP equation for the exact v_{xc} and making the quasiparticle approximation and an average orbital energy approximation, but *without* invoking the target Kohn-Sham approximation. The first term on the RHS of Eq. (A5) is the xc version of Slater's original (orbital-independent) local exchange potential [82] while the second term includes an orbital energy correction. In the exchange-only case, Eqs. (A4) and (A5) are identical, and reduce to the excellent approximation of Krieger, Li, and Iafrate [74,77].

- [1] I.E. McCarthy and E. Weigold, Rep. Prog. Phys. **51**, 299 (1988).
- [2] F.W. Byron, Jr. and C.J. Joachin, Phys. Rep. **179**, 211 (1989).
- [3] D. Feller, C.M. Boyle, and E.R. Davidson, J. Chem. Phys. **86**, 3424 (1987).
- [4] A.O. Bawagan, C.E. Brion, E.R. Davidson, and D. Feller, Chem. Phys. **113**, 19 (1987).
- [5] A.O. Bawagan, R. Müller-Fiedler, C.E. Brion, E.R. Davidson, and C. Boyle, Chem. Phys. **120**, 335 (1988).
- [6] C.L. French, C.E. Brion, and E.R. Davidson, Chem. Phys. **122**, 247 (1988).
- [7] S.A.C. Clark, E. Weigold, C.E. Brion, E.R. Davidson, R.F. Frey, C.M. Boyle, W. von Niessen, and J. Schirmer, Chem. Phys. **134**, 229 (1989).
- [8] S.A.C. Clark, C.E. Brion, E.R. Davidson, and C. Boyle, Chem. Phys. **136**, 55 (1989).
- [9] S.A.C. Clark, T.J. Reddish, C.E. Brion, E.R. Davidson, and R. Frey, Chem. Phys. **143**, 1 (1990).
- [10] E.R. Davidson, D. Feller, C.M. Boyle, L. Adamowicz, S.A.C. Clark, and C.E. Brion, Chem. Phys. **147**, 45 (1990).
- [11] B.P. Hollebhone, C.E. Brion, E.R. Davidson, and C. Boyle, Chem. Phys. **173**, 193 (1993).
- [12] P. Duffy, S.A.C. Clark, C.E. Brion, M.E. Casida, D.P. Chong, E.R. Davidson, and C. Maxwell, Chem. Phys. **165**, 183 (1992).
- [13] E.R. Davidson, C.M. Boyle, and R.F. Frey, in S.A. Clark Ph.D. thesis, University of British Columbia, 1990, pp. 15,129-132,136-140,149-151,161-162.
- [14] D.P. Chong, Chin. J. Phys. **30**, 115 (1992).
- [15] D.P. Chong, J. Chin. Chem. Soc. **39**, 375 (1992).
- [16] D.P. Chong and D. Papousek, J. Mol. Spectrosc. **155**, 167 (1992).
- [17] D.P. Chong and D. Papousek, Chem. Phys. Lett. **193**, 399 (1992).
- [18] D.P. Chong and D. Papousek, Chin. J. Phys. **30**, 829 (1992).
- [19] D.P. Chong and C.Y. Ng, J. Chem. Phys. **98**, 759 (1993).
- [20] D.P. Chong, D. Papousek, Y.-T. Chen, and P. Jensen, J. Chem. Phys. **98**, 1352 (1993).
- [21] D.P. Chong and A.V. Bree, Chem. Phys. Lett. **210**, 443 (1992).
- [22] P. Duffy, D.P. Chong, and M. Dupuis (unpublished).
- [23] D.P. Chong, Chem. Phys. Lett. **217**, 539 (1994).
- [24] D.P. Chong, Chem. Phys. Lett. **220**, 102 (1994).
- [25] N.L. Ma, W.-K. Li, D.P. Chong, and C.Y. Ng, Chem. Phys. **179**, 365 (1994).
- [26] J. Guan, P. Duffy, J.T. Carter, D.P. Chong, K.C. Casida, M.E. Casida, and M. Wrinn, J. Chem. Phys. **98**, 4753 (1993).
- [27] D. R. Salahub, M. Castro, and E. I. Proynov, in *Relativistic and Electron Correlation Effects in Molecules and Solids*, Vol. 318 of *NATO Advanced Study Institute, Series B: Physics*, edited by G.L. Malli (Plenum, New York, 1994).
- [28] D. R. Salahub et al., in *Theoretical and Computational Approaches to Interface Phenomena*, edited by H. Sellers and J.T. Golab (Plenum, New York, 1994).
- [29] W. Kohn and L.J. Sham, Phys. Rev. **140**, A1133 (1965).
- [30] R.T. Sharp and G.K. Horton, Phys. Rev. **90**, 317 (1953).
- [31] J.D. Talman and W.F. Shadwick, Phys. Rev. A **14**, 36 (1976).
- [32] L.J. Sham and M. Schlüter, Phys. Rev. Lett. **51**, 1888 (1983).
- [33] M.E. Casida (unpublished).
- [34] M.E. Casida and D.P. Chong, Chem. Phys. **132**, 391 (1989).
- [35] C.-O. Almbladh and U. von Barth, Phys. Rev. **31**, 3231 (1985).
- [36] M.E. Casida and D.P. Chong, Int. J. Quantum Chem. **40**, 225 (1991).
- [37] M.E. Casida and D.P. Chong, Phys. Rev. A **40**, 4837 (1989); **44**, 6151(E) (1991).
- [38] M.E. Casida and D.P. Chong, Phys. Rev. A **44**, 5773 (1991).
- [39] G.R.J. Williams, I.E. McCarthy, and E. Weigold, Chem. Phys. **22**, 281 (1977).
- [40] A.J. Dixon, I.E. McCarthy, E. Weigold, and G.R.J. Williams, J. Electron Spectrosc. **12**, 239 (1977).
- [41] A.J. Dixon, S.T. Hood, E. Weigold, and G.R.J. Williams, J. Electron Spectrosc. **14**, 267 (1978).
- [42] C.E. Brion, S.T. Hood, I.H. Suzuki, E. Weigold, and G.R.J. Williams, J. Electron Spectrosc. **21**, 71 (1980).
- [43] M.E. Casida and D.P. Chong, Chem. Phys. **133**, 47 (1989); **136**, 489(E) (1989).
- [44] A.J. Layzer, Phys. Rev. **129**, 897 (1963).
- [45] L.S. Cederbaum and W. Domcke, Adv. Chem. Phys. **36**, 205 (1977).
- [46] G.Y. Csanak, H.S. Taylor, and R. Yaris, Adv. At. Mol. Phys. **17**, 287 (1971).
- [47] J.D. Doll and W.P. Reinhardt, J. Chem. Phys. **57**, 1169 (1972).
- [48] M.F. Herman, K.F. Freed, and D.L. Yeager, Adv. Chem. Phys. **43**, 1 (1981).
- [49] Y. Öhrn and G. Born, Adv. Quantum Chem. **13**, 1 (1981).
- [50] W. von Niessen, J. Schirmer, and L.S. Cederbaum, Comput. Phys. Rep. **1**, 57 (1984).
- [51] B.T. Pickup and O. Goscinski, Mol. Phys. **26**, 1013 (1973).
- [52] M.S. Hybertsen and S.G. Louie, Phys. Rev. Lett. **55**, 1418 (1985).
- [53] M.S. Hybertsen and S.G. Louie, Phys. Rev. B **32**, 7005 (1985).
- [54] W. von der Linden, P. Horsch, and W.-D. Lukas, Solid State Commun. **59**, 485 (1986).
- [55] M.S. Hybertsen and S.G. Louie, Phys. Rev. B **34**, 5390 (1986).
- [56] R.W. Godby, M. Schlüter, and L.J. Sham, Phys. Rev. B **35**, 4170 (1987).
- [57] J.E. Northrup, M.S. Hybertsen, and S.G. Louie, Phys. Rev. Lett. **59**, 819 (1987).
- [58] M.S. Hybertsen and S.G. Louie, Adv. Quantum Chem. **21**, 155 (1990).
- [59] R.G. Parr and W. Yang, *Density-Functional Theory of Atoms and Molecules* (Oxford University Press, New York, 1989).
- [60] R.M. Dreizler and E.K.U. Gross, *Density Functional Theory* (Springer-Verlag, New York, 1990).
- [61] N.H. March, *Electron Density Theory of Atoms and Molecules* (Academic Press, New York, 1992).
- [62] P. Hohenberg and W. Kohn, Phys. Rev. **136**, B864 (1964).
- [63] M. Lanoo, M. Schlüter, and L.J. Sham, Phys. Rev. B **32**, 3890 (1985).
- [64] L.J. Sham and M. Schlüter, Phys. Rev. B **32**, 3883

- (1985).
- [65] L.J. Sham, Phys. Rev. B **32**, 3876 (1985).
- [66] R.W. Godby, M. Schlüter, and L.J. Sham, Phys. Rev. B **36**, 6497 (1987).
- [67] R.W. Godby, M. Schlüter, and L.J. Sham, Phys. Rev. B **37**, 10159 (1988).
- [68] M. Schlüter and L.J. Sham, Adv. Quantum Chem. **21**, 97 (1990).
- [69] M.M. Pant and J.D. Talman, Phys. Rev. A **17**, 1819 (1978).
- [70] M.M. Pant and J.D. Talman, Phys. Lett. **68A**, 154 (1978).
- [71] K. Aashamar, T.M. Luke, and J.D. Talman, At. Data Nucl. Data Tables **22**, 443 (1978).
- [72] K. Aashamar, T.M. Luke, and J.D. Talman, Phys. Rev. A **19**, 6 (1979).
- [73] J.D. Talman, P.S. Ganas, and A.E.S. Green, Int. J. Quantum Chem. Symp. **13**, 67 (1979).
- [74] J.B. Krieger, Y. Li, and G.J. Iafrate, Phys. Lett. A **146**, 256 (1990).
- [75] J.B. Krieger, Y. Li, and G.J. Iafrate, Phys. Lett. A **148**, 470 (1990).
- [76] Y. Li, J.B. Krieger, M.R. Norman, and G.J. Iafrate, Phys. Rev. B **44**, 10437 (1991).
- [77] J.B. Krieger, Y. Li, and G.J. Iafrate, Phys. Rev. A **45**, 101 (1992).
- [78] J.B. Krieger, Y. Li, and G.J. Iafrate, Int. J. Quantum Chem. **41**, 489 (1992).
- [79] Y. Li, J.B. Krieger, and G.J. Iafrate, Chem. Phys. Lett. **191**, 38 (1992).
- [80] Y. Li, J.B. Krieger, and G.J. Iafrate, Phys. Rev. A **47**, 165 (1993).
- [81] R.W. Godby, M. Schlüter, and L.J. Sham, Phys. Rev. Lett. **56**, 2415 (1986).
- [82] J.C. Slater, Phys. Rev. **85**, 385 (1951).
- [83] M.R. Norman and D.D. Koelling, Phys. Rev. B **30**, 5530 (1984).
- [84] J. D. Talman, Comput. Phys. Commun. **54**, 85 (1989).
- [85] Y. Wang, J.P. Perdew, J. Chevary, L.M. MacDonald, and S. Vosko, Phys. Rev. A **41**, 78 (1990).
- [86] J.P. Perdew and M. Levy, Phys. Rev. Lett. **51**, 1884 (1983).
- [87] Q. Zhao and R.G. Parr, Phys. Rev. A **46**, 2337 (1992).
- [88] Q. Zhao and R.G. Parr, J. Chem. Phys. **98**, 543 (1993).
- [89] L. Hedin, Phys. Rev. **139**, A796 (1965).
- [90] T. Koopmans, Physica **1**, 104 (1934).
- [91] J.C. Slater, Adv. Quantum Chem. **6**, 1 (1972).
- [92] J.F. Janak, Phys. Rev. B **18**, 7165 (1978).
- [93] P. Duffy and D.P. Chong, Org. Mass Spectrom. **28**, 321 (1993).
- [94] A. St.-Amant and D.R. Salahub, Chem. Phys. Lett. **387**, 387 (1990).
- [95] D.R. Salahub, R. Fournier, P. Mlanarski, I. Papai, A. St.-Amant, and J. Ushio, in *Density Functional Methods in Chemistry*, edited by J. Labanowski and J. Andzelm (Springer-Verlag, New York, 1991), p. 77.
- [96] A. St.-Amant, Ph.D. thesis, Université de Montréal, 1991.
- [97] E.R. Davidson, in *Modern Techniques in Computational Chemistry: MOTTECC-90*, edited by E. Clementi (ESCOM, Leiden, 1990), p. 417.
- [98] A.O. Bawagan, Ph.D. thesis, University of British Columbia, 1987, pp. 36–43.
- [99] J.C. Slater and J.H. Wood, Int. J. Quantum Chem. **4**, 3 (1971).
- [100] S.H. Vosko, L. Wilk, and M. Nusair, Can. J. Phys. **58**, 1200 (1980).
- [101] L. Fan and T. Ziegler, J. Chem. Phys. **94**, 6057 (1991).
- [102] A.D. Becke, Phys. Rev. A **38**, 3098 (1988).
- [103] J.P. Perdew, Phys. Rev. B **33**, 8822 (1986).
- [104] W.J. Hehre, R.F. Stewart, and J. Pople, J. Chem. Phys. **51**, 2657 (1969).
- [105] D. Neumann and J.W. Moscovitz, J. Chem. Phys. **49**, 2056 (1968).
- [106] J. Almlöf and P.R. Taylor, J. Chem. Phys. **87**, 4070 (1987).
- [107] G.D. Zeiss, W.R. Scott, N. Suzuki, D.P. Chong, and S.R. Langhoff, Mol. Phys. **37**, 1543 (1979).
- [108] P. Duffy, M.E. Casida, C.E. Brion, and D.P. Chong, Chem. Phys. **159**, 347 (1992).
- [109] C.J. Umrigar and X. Gonze, in *High Performance Computing and its Application to the Physical Sciences*, Proceedings of the Mardi Gras '93 Conference, edited by D.A. Browne *et al.* (World Scientific, Singapore, 1993), p. 43.
- [110] C.J. Umrigar and X. Gonze, Phys. Rev. A **50**, 3827 (1994).
- [111] D.P. Chong, J. Chin. Chem. Soc. **39**, 457 (1992).
- [112] M.J. Stott and E. Zaremba, Phys. Rev. A **21**, 12 (1980).
- [113] E.R. Davidson, Int. J. Quantum Chem. **37**, 811 (1990).
- [114] L.J. Sham and W. Kohn, Phys. Rev. **145**, 561 (1966).
- [115] Y. Zheng, J.J. Neville, C.E. Brion, Y. Wang, and E.R. Davidson, Chem. Phys. (to be published).
- [116] C.E. Brion *et al.* (private communication).
- [117] D. Feller and E.R. Davidson, Int. J. Quantum Chem. **54**, 489 (1984).
- [118] S.A. Clough, Y. Beers, G.P. Klein, and L.S. Rothman, J. Chem. Phys. **59**, 2254 (1973).
- [119] W.F. Murphy, J. Chem. Phys. **67**, 5877 (1977).
- [120] C.R. Brundle and D.W. Turner, Proc. R. Soc. London Ser. A **307**, 27 (1968).